Journal of the Meteorological Society of Japan

EARLY ONLINE RELEASE

This is a PDF of a manuscript that has been peer-reviewed and accepted for publication. As the article has not yet been formatted, copy edited or proofread, the final published version may be different from the early online release.

This pre-publication manuscript may be downloaded, distributed and used under the provisions of the Creative Commons Attribution 4.0 International (CC BY 4.0) license. It may be cited using the DOI below.

The DOI for this manuscript is
DOI:10.2151/jmsj.2021-074
J-STAGE Advance published date: September 9th, 2021
The final manuscript after publication will replace the preliminary version at the above DOI once it is available.

Comparative Evaluation of the Performances of TRMM-3B42 and CMORPH Precipitation Estimates over Thailand

Wen-Ting Yang

Laboratory of Cloud-Precipitation Physics and Severe Storms, Institute of Atmospheric Physics, Chinese Academy of Sciences, Beijing 100029, China

University of Chinese Academy of Sciences, Beijing 100049, China

Shen-Ming Fu#

International Center for Climate and Environment Sciences, Institute of Atmospheric Physics, Chinese Academy of Sciences, Beijing 100029, China

Jian-Hua Sun

Laboratory of Cloud-Precipitation Physics and Severe Storms, Institute of Atmospheric Physics, Chinese Academy of Sciences, Beijing 100029, China

Collaborative Innovation Center on Forecast and Evaluation of Meteorological Disasters, Nanjing University of Information Science and Technology, Nanjing 210044, China

Fei Zheng

International Center for Climate and Environment Sciences, Institute of Atmospheric Physics, Chinese Academy of Sciences, Beijing 100029, China

Jie Wei

Laboratory of Cloud-Precipitation Physics and Severe Storms, Institute of Atmospheric Physics, Chinese Academy of Sciences, Beijing 100029, China

and

Zheng Ma

Laboratory of Cloud-Precipitation Physics and Severe Storms, Institute of Atmospheric Physics, Chinese Academy of Sciences, Beijing 100029, China

Submitted to JMSJ on 2 December 2020 and revised on 25 August 2021

[#] Corresponding author: Shen-Ming Fu, International Center for Climate and Environment Sciences, Institute of Atmospheric Physics, Chinese Academy of Sciences, Beijing 100029, China. Email: fusm@mail.iap.ac.cn

Abstract

At present, satellite-derived precipitation estimates have been widely used as a supplement for the real precipitation observation. Detailed evaluations of a satellite precipitation estimate are the prerequisite for using it effectively. Based on the daily precipitation observation from 91 rain gauges throughout Thailand during a 15-yr period, this study evaluated the performances of daily precipitation data of CMORPH and TRMM (3B42 version 7) in an interpolating-grid-points-into-stations manner. This filled in the deficiencies of the current evaluations of TRMM-3B42v7's performances over Thailand, made the first evaluation of CMORPH in this region, and showed the first report of relative performances of two datasets.

For the entire Thailand, a total of 35 factors (including precipitation intensity, spatial distribution pattern, duration/interval) was used in the evaluation. It is found that only 12 of them (including annual and monthly variations of precipitation, conditional rain rate in rainy season, rainfall interval in entire year, non-precipitation days, etc.) were reproduced credibly (i.e., relative error was less than 20%) by the two datasets. Both TRMM-3B42v7 and CMORPH displayed similarly poor performances in representing intensity and spatial distribution of extreme precipitation. Comparisons based on the 35 factors indicate that TRMM-3B42v7 displayed a better overall performance than CMORPH for the entire Thailand.

For each region of Thailand, CMORPH/TRMM-3B42v7 showed different performances in different regions (a total of 19 factors was used). The CMORPH/TRMM-3B42v7 data made credible estimates over all five regions of Thailand in terms of daily precipitation intensity and monthly variation of precipitation, whereas, in terms of precipitation day fraction, conditional rain rate during dry season, and interval/duration of rainfall events during the rainy season, it showed notable errors in all regions. Overall, TRMM-3B42v7 exhibited superior performances to CMORPH for the North, Northeast, East, and South of Thailand, whereas, CMORPH and TRMM-3B42v7 displayed similar performances for the Central Thailand.

Keywords: TRMM-3B42v7; CMORPH; Precipitation evaluation; Thailand

1. Introduction

Thailand is situated on the Indochinese Peninsula and Malay Peninsula (Fig. 1), which is adjacent to the South China Sea in the east and the Indian Ocean in the west. It has a notable tropical monsoon climate, that features a high temperature throughout the year. Overall, the annual precipitation increases from north to south (Fig. 1): North, Northeast and Central Thailand mainly experience an annual precipitation of below 2000 mm, whereas, that of East and South Thailand is mainly above 2000 mm, with 2 stations exceeding 4000 mm. Strong precipitation primarily appears from May to September, during which the southwest monsoon is active over Thailand (Chokngamwong and Chiu, 2008).

According to statistics, Thailand is the largest producer and exporters of rice in the world (John 2013; Promchote et al. 2016), and thus it plays an important role in ensuring the global food security. As the rice yield is heavily dependent on precipitation, for years, great efforts had been made to further the understanding of precipitation features over Thailand. Thus far, most of the related studies were conducted by using the rain gauge (RG) observed precipitation (Cheong et al. 2018; Manomaiphiboon et al. 2013; Torsri et al. 2013; Tangang et al. 2019). However, since the RG observed precipitation data is notably limited by the spatial distribution and density of the ground observation stations (Huang et al. 2016; Morrissey et al. 1995), key features of the precipitation over Thailand remains to be further deepened. With the development of satellite remote sensing, the satellite-derived precipitation estimates with high spatial and temporal resolution became an effective supplement for the RG-based precipitation (Huang et al. 2016; Schulz et al. 2009). Nevertheless, all satellite precipitation data is associated with uncertainties related to its detection mode and retrieval algorithms, which notably reduce their accuracy (Nair et al. 2009). Therefore, before using a type of satellite precipitation data for a specific research or application, it is necessary to first know its advantages and limitations. This means that a detailed evaluation of the satellite precipitation data is of paramount importance. Moreover, the evaluation is also a prerequisite for improving the retrieval algorithms of satellites (Belete et al. 2020; Kidd et al. 2012; Xu et al. 2017).

Previous studies had evaluated several aspects of the satellite precipitation data over Thailand. For instance, Chokngamwong and Chiu (2008) used a 10-yr RG-observed daily precipitation data over Thailand to evaluate the daily satellite precipitation data from the Tropical Rainfall Measuring Mission (TRMM; 3B42v5 and 3B42v6) (Huffman et al. 2007). The authors found that the satellite precipitation data mainly overestimated the rainfall events' duration. Veerakachen et al. (2014) evaluated the performance of Global Satellite Mapping of Precipitation (GSMaP) products over the Chaophraya River basin of Thailand and found that GSMap_NRT (Near Real Time) data underestimated the rain rate. Li et al. (2019) evaluated the TRMM-3B42v7 precipitation data over the Mun-chi River Basin in Thailand and found that the data was capable of monitoring the night-day rainfall diurnal cycle in this region and it could provide useful near real-time flood information for risk management. Kim et al. (2019) compared RG-based, satellite-based, and reanalysis-based precipitation data over a 10-yr period. They found that the three types of datasets showed notable differences in displaying precipitation extremes over the Southeast Asia including Thailand.

As mentioned above, previous studies had demonstrated that the TRMM precipitation data can provide credible estimates of the real precipitation over Thailand in some aspects.

However, these studies had not evaluated performances of the TRMM-3B42v7 precipitation data in representing regional precipitation trends and monthly to yearly precipitation features over Thailand. These are crucial for obtaining a comprehensive understanding of the precipitation over Thailand. Currently, there is another type of widely used satellite precipitation data, namely, the National Oceanic and Atmospheric Administration/Climate Prediction Centre (NOAA/CPC) morphing technique (CMORPH) precipitation data (Joyce et al. 2004). This dataset had been found to be effective for representing key features of precipitation in numerous regions (Babaousmail et al. 2019; Chua et al. 2020; Soo et al. 2020; Villanueva et al. 2018; Yang et al. 2020). However, to the best of our knowledge, no studies had yet evaluated the performance of CMORPH over Thailand, nor had any studies compared the performances of TRMM-3B42v7 and CMORPH over Thailand. In an effort to fill this research gap, the goal of the present study was to conduct a detailed comparative evaluation of the performances of TRMM-3B42v7 and CMORPH over Thailand during a 15-yr period (longer than the periods used in most similar studies). Multiple aspects (including regional, seasonal, and monthly and daily precipitation features, etc.) were evaluated in this study to provide a reliable reference for future studies and policy makers.

The remainder of this manuscript is organized as follows: Section 2 describes the data and methods, Sections 3–6 present the evaluated precipitation intensity, spatial distribution pattern, duration/interval, and other features, and Section 7 provides the overall conclusions.

2. Data and methods

2.1. Dataset

In this study, three types of data were used in total: (i) Daily precipitation data from RGs at

120 observational stations throughout Thailand, which were provided by the Thailand Meteorological Department (TMD). Upon verification, it was found that only 91 (Fig. 1) of the 120 stations provided a sufficiently complete (i.e., missing data does not exceed 5% of the total data amount) precipitation series from 1998 to 2012. These 91 stations were independent of the rain gauge data used in TRMM-3B42v7 and CMORPH precipitation estimates. (ii) The 0.25°×0.25° TRMM-3B42v7 gridded daily precipitation product in the domain 50°N-50°S (Chen et al. 2013) from 1998 to 2012 provided by the National Aeronautics and Space Administration (NASA). This new version (v7) data fully utilizes various available detection data provided by the satellite sensors (including microwave TRMM Microwave Imager, TRMM Combined Instrument, Special Sensor Microwave Imager, etc.) and gauges to permit credible precipitation estimates (Huffman et al. 2007; Li et al. 2019). (iii) The 0.25°×0.25° CMORPH daily global precipitation product from 1998 to 2012, which was developed by the NOAA (Joyce et al. 2004). This data is generated by a Morphing technology, based on the passive microwave and infrared precipitation observation. At present, there are a total of three types of daily CMORPH precipitation data: (i) the raw, satellite only precipitation data; (ii) the bias corrected (CRT) precipitation data; and (iii) the gauge-satellite blended (BLD) precipitation data. In this study, the bias corrected (CRT) version was used, as it showed credible performances in various aspects (https://climatedataguide.ucar.edu/climate-data/cmorph-cpc-morphing-technique-high-resolution-precipitation-60s-60n).

2.2. Methods

There are five administrative districts of Thailand (with the 91 available observational stations distributed unevenly within these regions): the northern, northeastern, central, eastern, and southern regions (Chokngamwong and Chiu 2008). From Fig. 1, it is clear that the geographic features of these regions are notably different from each other: (i) the northern region is mountainous, which has the highest altitude among all the five regions; (ii) the northeast region is mainly a plateau, which has the second highest altitude; (iii) the central region is mainly a plain, which has a low altitude; (iv) the eastern region faces the Gulf of Thailand on its southern side; and (v) the southern region is significantly different from the other four regions as it borders oceans on its both sides. Different geographic features will lead to different precipitation features, implying that each region needs a detailed analysis.

To compare the RG observation with satellite precipitation, it is necessary to reform the three types of data to a same format. In order to minimize the uncertainties during the process of reformatting data, we interpolated the 0.25°×0.25° satellite data into the 91 stations using the bilinear interpolation method (Mastylo, 2013). This is because that the 91 stations are too sparse for generating a credible 0.25°×0.25° grided precipitation dataset over Thailand, whereas, the 0.25°×0.25°grided precipitation is of credibility to produce the station precipitation data at the 91 stations over Thailand. Key features of a rainfall event mainly contain three aspects: the intensity, the spatial distribution pattern and the duration. These were evaluated quantitatively using the methods described below.

a. INTENSITY EVALUATION

Intensity evaluation was conducted on different temporal scales including the 15-yr period, annual, seasonal (i.e., rainy and dry seasons), monthly and daily scales. The mean daily precipitation intensity at a particular station was defined as the accumulated precipitation at that station divided by the total number of days during the 15-yr period. The conditional rain rate (CRR) for a station was defined as the temporal average of daily precipitation intensity for all of the days when the precipitation at that station was above 0 mm (Chokngamwong and Chiu 2008).

The bias (BIAS), root-mean-square difference (RMSD), and mean absolute difference (MAD) were used to evaluate the ability of TRMM-3B42v7 and CMORPH to represent the rainfall intensity at each station during the 15-yr period. These parameters were defined as follows:

$$\mathrm{BIAS} = \frac{1}{n}\sum_{i}(x_i - \mathrm{RG}_i) \quad (1),$$

$$\mathrm{RMSD} = \sqrt{\frac{1}{n}\sum_{i}(x_i - \mathrm{RG}_i)^2} \quad (2),$$

$$\mathrm{MAD} = \frac{1}{n}\sum_{i}\left|x_i - \mathrm{RG}_i\right| \quad (3),$$

For the case of 15-yr overall features of precipitation intensity evaluation, n is the total number of days (5479), x_i is the daily satellite precipitation estimate, RG_i is the RG observation for the station, and the subscript i denotes time. For the case of evaluating the 15-yr precipitation linear trend, x_i and RG_i denote the 15-yr linear trends of precipitation at station i (subscript i denotes the station number, and n = 91) derived from satellite data and RG observation, respectively.

b. SPATIAL DISTRIBUTION PATTERN EVALUATION

Skill measures including the false alarm rate (FAR) (Eq. (4)), probability of detection (POD) (Eq. (5)), and critical success index (CSI) (Eq. (6)) were calculated to evaluate the satellite precipitation data (Schaefer 1990). As shown in Table 1, V_a and V_d denote the numbers of stations where the satellite data correctly estimated the situation of precipitation and non-precipitation (without taking the precipitation intensity into consideration), respectively. V_b is the number of stations where the satellite data did not reproduce the real precipitation (i.e., it missed), and V_c represents the number of stations where the satellite incorrectly estimated a rainfall as precipitation did not occur (i.e., false alarm).

$$\mathrm{FAR} = \frac{V_c}{V_a + V_c} \quad (4),$$

$$\mathrm{POD} = \frac{V_a}{V_a + V_b} \quad (5),$$

$$\mathrm{CSI} = \frac{V_a}{V_a + V_b + V_c} \quad (6),$$

As documented by Schaefer (1990), the FAR represents the proportion of rainfall events estimated from the satellite data that are false alarms relative to all rainfall events derived from the data, the POD represents the proportion of rainfall events that are estimated correctly from the satellite data relative to all real rainfall events, and the CSI represents the proportion of rainfall events that are estimated correctly by the satellite data relative to all rainfall events. The difference between the POD and the CSI is mainly caused by false alarms (V_c in Table 1). Comprehensive analysis of the FAR, POD, and CSI can reveal the ability of satellite data to reproduce the spatial distribution patterns of real rainfall events (considering only precipitation and non-precipitation, without considering precipitation intensity).

To consider the precipitation intensity while evaluating the performance of satellite data in reproducing the spatial distribution patterns of real rainfall events, spatial correlation between satellite data (CMORPH/TRMM-3B42v7) and RG observation was calculated. The spatial correlation could be used to directly evaluate the spatial similarity between the satellite data and RG observations, and it was calculated as follows. First, we determined all the days during which ≥10 stations (of the total 91 stations) had a daily precipitation exceeding 0 mm, and then for each selected day (4113 days of the total 5479 days) we calculated the correlation between the satellite data and RG observations for 91 stations.

c. DURATION/INTERVAL EVALUATION

The duration of a precipitation event at a station was defined as the number of consecutive days during which the precipitation at that station exceeded 0 mm. The interval of two adjacent precipitation events at a station was defined as the number of consecutive days between the two precipitation events during which there was no precipitation at that station.

d. OTHER FEATURES

How a precipitation dataset depends on its past is an important quality index (Chokngamwong and Chiu 2008). In this study, autocorrelation was used to evaluate this feature. The lower the autocorrelation is, the less likely the detection data is dependent on the possible regularity of the past detection data. Moreover, autocorrelation is also useful for assessing the stationarity of data, as a stationary data typically exhibits short-term autocorrelation (Yu et al. 2007). In this study, the autocorrelation was calculated as follows:

$$\rho(\tau)=\frac{[X(s,t)X(s,t+\tau)]\text{-}[X][X]}{{\sigma_X}^2} \qquad (7),$$

where $\rho(\tau)$ represents the temporal autocorrelation coefficient when the temporal lag is τ (days; τ=1,…,20,); $X(s, t)$ is the precipitation intensity, with s representing a station and t denoting a time; [] indicates ensemble averaging over all spatial and temporal samples; and σ_X denotes the standard deviation of X.

In order to judge whether the results derived from the satellite data were credible, the relative error (RE) was developed as the following shown:

$$RE = \frac{P_{\text{satellite}} - P_{\text{real}}}{P_{\text{real}}} \quad (8),$$

where $P_{\text{satellite}}$ is a feature that is derived from the satellite precipitation data, and P_{real} is the same feature derived from the RG-observed precipitation. The RE indicates the percentage of the error relative to the real value. If the RE of a feature (e.g., precipitation intensity, duration, etc.) is less than 20%, it is regarded that the satellite data produces this feature credibly (for the spatial distribution pattern, "credibly" means FAR<0.2 and POD≥0.8), otherwise, it is uncredible.

3. Precipitation intensity evaluation

3.1. 15-yr overall features

According to the RG observations, over the whole Thailand during the 15-yr period, the mean daily precipitation intensity was ~4.5 mm day^{-1} (Table 2), the mean CRR was ~12 mm day^{-1}, and the precipitation day fraction (PDF; the number of precipitation days divided by the total number of days) was ~36%. Both CMORPH and TRMM-3B42v7 underestimated the mean CRR (with RE values of approximately −42% and −27%, respectively) and overestimated the PDF (with RE values of approximately 61% and 44%, respectively). The mean daily precipitation was underestimated by CMORPH and overestimated by TRMM-3B42v7 (with RE values of approximately −8% and 3%, respectively). Among the five regions, East and South Thailand had the highest mean daily precipitation intensity and CRR (Table 2). For these two regions, CMORPH and TRMM-3B42v7 displayed similar performances as those for the whole Thailand with respect to the mean CRR and PDF. The mean daily precipitation intensity was underestimated by both CMORPH and TRMM-3B42v7, with TRMM-3B42v7 exhibiting a smaller absolute RE value. For North and

Northeast Thailand, the performances of CMORPH and TRMM-3B42v7 were similar to those for the whole Thailand in all three aspects (Table 2). For Central Thailand, which had the lowest mean daily precipitation intensity, the performances of CMORPH and TRMM-3B42v7 were similar to those of the whole Thailand with respect to the mean CRR and PDF. However, both CMORPH and TRMM-3B42v7 overestimated the mean daily precipitation intensity. As discussed above, TRMM-3B42v7 and CMORPH afforded the most credible estimate for the mean daily precipitation intensity and the least credible estimate for the PDF. This was also evidenced in Section 3.5 as both types of satellite data did not satisfactorily reproduce the number of non-precipitation days. PDF also indicated that both satellite data overestimated the frequency of precipitation events, with TRMM-3B42v7 being closer to RG observations. Overall, compared to CMORPH, TRMM-3B42v7 exhibited superior performance, except for the mean daily precipitation intensity over Central Thailand (Table 2).

Over the whole Thailand during the 15-yr period (5479 days), the BIAS values for CMORPH and TRMM-3B42v7 were −0.36 and 0.15 mm day^{-1}, respectively (Table 3), which indicates that CMORPH/TRMM-3B42v7 underestimated/overestimated the precipitation intensity. TRMM-3B42v7 displayed a better performance. This is consistent with the situation regarding the mean daily precipitation intensity (Table 2). In terms of MAD and RMSD, CMORPH exhibited better performance than TRMM-3B42v7 (Table 3). Among all five regions, in terms of the MAD and RMSD, the situations were similar to those for the whole Thailand, with CMORPH having better performance. However, with respect to the BIAS values, only North and Northeast Thailand showed similar situations to those for the whole Thailand. In contrast, CMORPH overestimated the precipitation intensity in Central Thailand

and TRMM-3B42v7 underestimated that in East and South Thailand. For both types of satellite precipitation, their MAD and RMSD were comparable to their mean daily precipitation intensity (Table 2), which means they showed obvious errors in representing the precipitation intensity. Overall, in terms of BIAS, TRMM-3B42v7 displayed a better performance than CMORPH (Table 3), whereas for MAD and RMSD, CMORPH was better.

3.2. Annual precipitation evaluation

The annual (accumulated) precipitation at each of the 91 available stations (Fig. 1) was calculated using the three types of precipitation data and then averaged for each region. The results are presented in Fig. 2. It was found that, for the whole Thailand, both CMORPH and TRMM-3B42v7 had captured the key variation features of the RG-observed precipitation (Fig. 2a), as their respective correlation coefficients with the observed precipitation exceeded 0.98. TRMM-3B42v7 overestimated the annual precipitation with a mean RE of ~3% (Fig. 3a), whereas CMORPH underestimated the annual precipitation with a mean RE of ~8%. This indicates that both TRMM-3B42v7 and CMORPH perform well on providing relatively credible quantitative estimates of the annual precipitation over Thailand.

Similar result characteristics to Figs. 2a and 3a were also observed for North and Northeast Thailand (Figs. 2c, 2e, 3c, and 3e), where both types of satellite data captured the key variation features and afforded relatively credible quantitative estimates of the annual precipitation, with TRMM-3B42v7 displaying better performance than CMORPH.

For Central Thailand, both CMORPH and TRMM-3B42v7 reproduced the main annual precipitation variation features of the RG-observed precipitation, with TRMM-3B42v7 affording a higher correlation coefficient (Fig. 2b). Both types of satellite data overestimated the precipitation, with mean RE values of ~6% and ~18% for CMORPH and TRMM-3B42v7, respectively (Fig. 3b). This indicates that CMORPH afforded a much more credible quantitative estimate of the annual precipitation for this region.

For South and East Thailand, TRMM-3B42v7 satisfactorily reproduced the key variation of real annual precipitation (both correlation coefficients were above 0.94), whereas CMORPH only captured the key variation for South Thailand with a correlation coefficient of ~0.94 (Fig. 2d). Both types of satellite data underestimated the precipitation, with TRMM-3B42v7 affording mean RE values of approximately −10% over East Thailand and −6% over South Thailand and CMORPH affording mean RE values of approximately −18% over East Thailand and −11% over South Thailand. Therefore, for South and East Thailand, TRMM-3B42v7 captured the key variation features and provided credible quantitative estimates of the annual precipitation. In contrast, CMORPH displayed relatively poor performance in terms of both variation features and intensity for East Thailand (Figs. 2f and 3f), whereas its performance was credible for South Thailand (although inferior to that of TRMM-3B42v7).

As described above, TRMM-3B42v7 displayed better performance in reproducing the variation features of annual precipitation than CMORPH for all regions. TRMM-3B42v7 provided a more credible annual precipitation estimate than CMORPH for all regions except Central Thailand.

3.3. Monthly precipitation evaluation

The monthly (accumulated) precipitation at each of the 91 available stations (Fig. 1) was averaged during the 15-yr period (from 1998 to 2012) using the three types of data. The resulting monthly precipitation was then averaged within the different regions to reveal their respective overall characteristics. As shown in Fig. 4a, over the whole of Thailand, the monthly precipitation from May to October was much heavier than that in the other months. This is consistent with the onset and retreat of the Asian monsoon system and the displacement of the intertropical convergence zone rainband (Chokngamwong and Chiu 2008; Ding et al. 2018; Tangang et al. 2019). Both types of satellite precipitation data captured the key features of the monthly precipitation variation (Fig. 4a). However, TRMM-3B42v7 overestimated the precipitation intensity from May to October with a mean RE of ~6% (Fig. 5a), whereas in other months it mainly underestimated the precipitation intensity with a mean RE of approximately −10%. The types of major rain clouds in different seasons affect the performance of TRMM-3B42v7 precipitation estimate notably: studies have shown that the organized stratiform rain may cause TRMM Microwave Imager (TMI) to overestimate precipitation, while deep-isolated rain may result in underestimation (Sekaranom and Masunaga 2018). Meanwhile, CMORPH underestimated the monthly precipitation in all 12 months (Fig. 5a), particularly during the months with lighter precipitation (i.e., November to April) with a mean RE of approximately −14%, whereas in the other months it underestimated the monthly precipitation with a mean RE of approximately −7%. Therefore, both types of satellite data provided credible quantitative estimates of the monthly precipitation over the whole of Thailand, with TRMM-3B42v7 displaying better performance than CMORPH.

Similar monthly precipitation variations to those for the whole Thailand were observed for Central, North, Northeast, and East Thailand (Figs. 4b, 4c, 4e, and 4f), where both types of satellite data captured the main variation features of the real precipitation. However, the performances of CMORPH and TRMM-3B42v7 were different. For Central Thailand, TRMM-3B42v7 overestimated the precipitation from May to September with a mean RE of ~11% (Fig. 5b), whereas in the other months it generally underestimated the precipitation with a mean RE of approximately −25%. Meanwhile, CMORPH overestimated the precipitation in March, April, May, June, July, August, September, and December with a mean RE of ~9% (Fig. 5b), whereas it underestimated the precipitation in other months with a mean RE of approximately −6%. Therefore, with respect to the monthly precipitation over Central Thailand, CMORPH showed better performance than TRMM-3B42v7. For North and Northeast Thailand, TRMM-3B42v7 overestimated the precipitation from March to October with a mean RE of ~7% (Figs. 5c and 5e), whereas it underestimated the precipitation in other months with mean RE values of approximately −12% in North Thailand and −5% in Northeast Thailand. Meanwhile, CMORPH mainly underestimated the precipitation for North and Northeast Thailand (except for December in Northeast Thailand) with a mean RE of approximately −12% for both regions (Figs. 5c and 5e). Therefore, for the monthly precipitation over North and Northeast Thailand, TRMM-3B42v7 displayed better overall performance than CMORPH. For East Thailand, both types of satellite data underestimated the monthly precipitation (Fig. 5f). For the period from February to October, TRMM-3B42v7 afforded a lower RE for each month than CMORPH, whereas in the other three months the RE values were smaller for CMORPH. Overall, TRMM-3B42v7 displayed better performance than CMORPH for the monthly precipitation over East Thailand.

South Thailand exhibited monthly precipitation variation features that were clearly different to those for the whole Thailand (Figs. 4a and 4d), as it is situated in a notably different location compared with the other regions of Thailand (Fig. 1). For this region, heavier monthly precipitation was mainly found from May to December (Fig. 4d). Both types of satellite data captured the key variation features of the real precipitation (Fig. 4d). Both TRMM-3B42v7 and CMORPH mainly underestimated the monthly precipitation with the exception of TRMM-3B42v7 in April and July (Fig. 5d), with CMORPH exhibiting larger absolute RE values. This indicates that TRMM-3B42v7 displayed better performance than CMORPH for this region.

3.4. Evaluation of rainy and dry seasons

As discussed in Section 3.3, the rainy season (i.e., the months with considerably higher monthly precipitation than other months) occurred from May to October for Thailand as a whole, Central Thailand, and East Thailand (Fig. 4), from May to September for North and Northeast Thailand, and from May to December for South Thailand. For each region, the months other than those belonging to the rainy season were considered to constitute the dry season. The mean CRR values associated with daily precipitation intensity for the rainy and dry seasons of each region during the 15-yr period were calculated and are presented in Fig. 6. According to the RG observations, the mean CRR values for each region were highest in the rainy season and lowest in the dry season (Fig. 6a). However, the differences between the mean CRR values for the rainy and dry seasons were not noticeable (for Thailand as a whole, the difference was ~2 mm day^{-1}), which indicates that the notable differences in the accumulated precipitation between the two seasons were mainly attributable to the precipitation frequency.

As shown in Figs. 6b and 6c, both types of satellite data underestimated the mean CRR values for all regions during the three periods (rainy season, dry season and entire year). These underestimates were more obvious for the dry season than for the rainy season. TRMM-3B42v7 exhibited superior performance in representing the mean CRR values for all regions and all three periods, particularly for the rainy season, as its percentages to the real mean CRR values were approximately 80% (Fig. 6c). Therefore, TRMM-3B42v7 performs well in providing relatively credible estimates of the mean CRR values during the rainy season for all regions. In contrast, CMORPH only reproduced ~60% of the real mean CRR values for all regions, which corresponds to notable underestimation.

3.5. Daily precipitation evaluation

Cumulative distribution functions can be used to describe the distribution features of precipitation intensity (Kolmogorov 1933; Smirnov 1948). The cumulative distribution functions of the daily precipitation data at the 91 stations during the 15-yr period (498,589 samples for each dataset) are presented in Fig. 7. Percentages of zero precipitation samples to total samples were 64%, 42%, and 48% for the RG, CMORPH, and TRMM-3B42v7 data, respectively. This means that both types of satellite data underestimated the number of non-precipitation days by ~20%, which means that they did not satisfactorily reproduce the number of non-precipitation days. The TRMM-3B42v7 curve was always below the CMORPH curve when the rainfall exceeded 1 mm day^{-1}, indicating that TRMM-3B42v7 mainly showed a larger proportion of days with rainfall above 1 mm day^{-1}. The CMORPH and RG curves intersected at ~10 mm day^{-1}, which indicates that the proportion of days with daily precipitation above 10 mm was the same for RG and CMORPH (~13% of total rainfall events). Similarly, the TRMM-3B42v7 and RG curves intersected at ~18 mm day^{-1}, and thus the proportion of days with daily precipitation above 18 mm was the same for RG and TRMM-3B42v7 (~8% of total rainfall events).

According to the precipitation intensity classification scheme of the Chinese Meteorological Administration, 0.1 mm ≤ daily precipitation < 10 mm is defined as light rainfall, 10 mm ≤ daily precipitation < 25 mm is defined as moderate rainfall, 25 mm ≤ daily precipitation < 50 mm is defined as heavy rainfall, and daily precipitation ≥ 50 mm is defined as torrential rainfall. From Fig. 7, it is clear that the proportion of days with a daily precipitation of <10 mm, which includes no rainfall and light rainfall, was similar for the three datasets (the proportions from CMORPH and TRMM-3B42v7 accounted for ~100% and ~98% of that from RG). The proportion of days with moderate rainfall was overestimated by both types of satellite data, with CMORPH closer to RG than TRMM-3B42v7. For heavy rainfall, TRMM-3B42v7 was close to RG, whereas CMORPH afforded an underestimate. The proportion of days with torrential rainfall was underestimated by both types of satellite data, with TRMM-3B42v7 and CMORPH accounting for 66% and 57%, respectively, of the RG data. Overall, for non-precipitation days and light, heavy, and torrential rainfall, TRMM-3B42v7 displayed better performance, whereas CMORPH was superior for moderate rainfall.

3.6. Evaluation of extreme rainfall and different temporal scales

As discussed in Section 3.5, both types of satellite data notably underestimated the proportion of torrential rainfall events. In terms of extreme precipitation (first 5% in the ranking of precipitation intensity based on total samples at the 91 stations, i.e., precipitation above the 95th percentile), both types of satellite data considerably underestimated the intensity (Fig. 8). TRMM-3B42v7 only reproduced the intensity of 25% of these torrential rainfall events to above 75% of the real precipitation intensity. Among these, some events were overestimated by up to six times. For ~50% of the torrential rainfall events, TRMM-3B42v7 only reproduced their intensity to below 41%. Compared to TRMM-3B42v7, CMORPH displayed even worse performance, as it only reproduced the intensity of 25% of the torrential rainfall events to above 70% (some events were overestimated by up to six times), while for ~50% of the torrential rainfall events it only reproduced their intensity to below 37%.

As 5- and 10-d averaged rain rates are useful for meteorology, agriculture, and hydrology (Chokngamwong and Chiu 2008), we calculated the linear correlation coefficients between the running means of the RG and satellite data (CMORPH/TRMM-3B42v7) for all 91 stations and then calculated their average over the whole of Thailand. From Fig. 9, it can be seen that, from the daily to monthly (30 days) scale, the correlations between both type of satellite data and the RG precipitation data increased. This indicates that the performance improved with increasing temporal scale for both types of satellite data. With respect to the daily precipitation, both types of satellite data exhibited almost the same correlation coefficient of ~0.55. For the 5-d precipitation, the correlation coefficients for CMORPH and TRMM-3B42v7 were ~0.7 and ~0.72, respectively, while for the 10-d precipitation, the correlation coefficients for CMORPH and TRMM-3B42v7 were ~0.77 and ~0.79, respectively. For the monthly precipitation, the correlation coefficients for CMORPH and TRMM-3B42v7 were ~0.86 and ~0.89, respectively. Therefore, TRMM-3B42v7 displayed slightly better performance than CMORPH and both types of satellite data afforded credible estimates for temporal scales of 10 d or longer.

4. Evaluation of precipitation spatial distribution patterns over Thailand

4.1. 15-yr overall features

As shown in Table 4, over the entire year, the POD and FAR values for both types of satellite data were ≥0.88 and ≥0.39, respectively, which indicates a low missing rate and notable false alarm rate in both cases. The CSI values for both types of satellite data were comparable at ≥0.55, which indicates a similar performance in reproducing the real spatial distribution patterns of real rainfall events only considering precipitation and non-precipitation. The POD value for CMORPH was higher than that for TRMM-3B42v7 (Table 4), whereas the CSI value was lower, which indicates that CMORPH had a lower missing rate in reproducing the real precipitation but also a higher false alarm rate compared to TRMM-3B42v7. This was further confirmed by the higher FAR of CMORPH.

In consideration of the precipitation intensity, the spatial correlation between the satellite data and RG observations was calculated. The results are presented in Fig. 10. In this figure, the top and bottom boundaries of the blue boxes represent the 75th and 25th percentiles, respectively, where the spatial correlation coefficients above the 25th percentiles are statistically significant above the 99% confidence level. As shown in Fig. 10, the whiskers for both types of satellite data revealed similar ranges, the median values were the same, and the 75th/25th percentiles were close to each other. These results indicate that there was no significant difference between CMORPH and TRMM-3B42v7 in representing the spatial distribution pattern of real rainfall events. Furthermore, for both types of satellite data, over

50% of the spatial correlation coefficients were below 0.47 (i.e., 47% similarity), which indicates that both CMORPH and TRMM-3B42v7 gave notable errors in representing the spatial distribution patterns of real precipitation events.

4.2. Evaluation of different temporal scales

On the seasonal scale, in four seasons (winter, spring, summer and autumn), both types of satellite data afforded similar CSI values (Table 4), whereas the POD and FAR values were larger for CMORPH. This indicates that both types of satellite data displayed similar performance in reproducing the spatial distribution patterns of real rainfall events; however, compared to TRMM-3B42v7, CMORPH had a lower missing rate but also a higher false alarm rate. In addition, both types of satellite data exhibited better performance from March to November than in December, January, and February.

For daily to monthly temporal scales, the variation features of the CMORPH/TRMM-3B42v7 CSI curves (Fig. 11) were similar to those shown in Fig. 9, i.e., both types of satellite data exhibited better performance for longer temporal scales. However, in contrast to the situation depicted in Fig. 9, the CSI values for CMORPH and TRMM-3B42v7 were close to each other (Fig. 11), i.e., approximately 0.56 for daily precipitation, ~0.79 for 5-d precipitation, ~0.85 for 10-d precipitation, and ~0.92 for monthly precipitation.

Comparison of Figs. 9 and 11 revealed that both types of satellite data exhibited better performance in reproducing the spatial distribution patterns of rainfall over Thailand than in reproducing its intensity features. Overall, TRMM-3B42v7 displayed better performance in reproducing the intensity of multi-temporal scale rainfall, whereas the ability to reproduce spatial features was similar for both types of satellite data. For temporal scales of 10 d or longer, both types of satellite data provided credible estimates of the spatial distribution pattern and intensity of precipitation.

4.3. Evaluation for different precipitation intensities

For both types of satellite data, the POD and CSI values decreased rapidly as the precipitation intensity increased from 0 to 10 mm day^{-1} (the precipitation intensity thresholds were applied to the gauges), moderately as it increased from 10 to 20 mm day^{-1}, and slowly as it increased from 20 to 30 mm day^{-1} (Fig. 12). The situations of FAR was similar to those of POD and CSI, whereas the trend was upward. The POD and CSI values for both types of satellite data decreased with increasing precipitation intensity, which indicates that the ability to reproduce the spatial distribution patterns of rainfall became weaker as the precipitation intensity increased. The POD and CSI curves for TRMM-3B42v7 were generally higher than those for CMORPH, which indicates that TRMM-3B42v7 displayed better performance than CMORPH. However, Table 4 also shows that CMORPH displayed a higher POD than TRMM-3B42v7 over all seasons. This apparent discrepancy between Fig. 12 and Table 4 can be attributed to the fact that CMORPH displayed a higher POD when the precipitation intensity was less than 1 mm day^{-1}, which accounted for a large proportion of all rainfall intensities (Fig. 7).

For both types of satellite data, the FAR increased with increasing precipitation intensity (Fig. 12). This indicates that the number of false alarms increased as the rainfall intensity increased, i.e., the performance became worse for both types of satellite data. The FAR curve for CMORPH was higher than that for TRMM-3B42v7, which indicates that TRMM-3B42v7 displayed better performance than CMORPH. This is consistent with the results shown in Table 4.

5. Duration and interval evaluation

As discussed in Section 3.3, the performance of the satellite data varied both seasonally and regionally. In this section, we focus on the ability of CMORPH and TRMM-3B42v7 to reproduce the duration and interval of precipitation events within each region during the rainy and dry seasons. The mean duration and interval for each region in its respective rainy and dry seasons during the 15-yr period were calculated as shown in Fig. 13.

According to the RG observations, over the whole of Thailand, the mean interval of rainfall events was ~5 d during the entire year (Fig. 13a), ~2.5 d during the rainy season, and ~11 d during the dry season. All of the individual regions showed similar features, with the exception of South Thailand owing to its notably different rainy season. Both types of satellite data underestimated the mean interval for all regions, with the estimates for the entire year and the rainy season accounting for over 70% of the RG values (Figs. 13c and 13e). With respect to the mean interval during the entire year, CMORPH displayed better performance for Thailand as a whole and North, Northeast, and Central Thailand, whereas it displayed worse performance for East and South Thailand. With respect to the mean interval during the rainy season, TRMM-3B42v7 displayed better performance than CMORPH for regions. With respect to the mean interval during the dry season, CMORPH exhibited superior performance for North and Northeast Thailand and inferior performance for Central, East, and South Thailand, whereas both types of satellite data showed comparable performance for Thailand as a whole.

Over all regions, the mean duration of RG-observed rainfall events was ~3 d during the entire year and the rainy season (Fig. 13b) and ~2 d during the dry season. Both types of satellite data overestimated the mean duration, with the largest and smallest overestimates occurring for the rainy season and dry season, respectively (Figs. 13d and 13f). The mean duration estimates by CMORPH and TRMM-3B42v7 were mainly higher than the real situation, with TRMM-3B42v7 making credible estimates in the Central, East and South Thailand. Overall, for all regions and all three periods, TRMM-3B42v7 displayed better performance than CMORPH in representing the mean duration.

6. Autocorrelation and 15-yr trend evaluation

On the basis of Eq. (8), the temporal autocorrelation functions for RG, CMORPH, and TRMM-3B42v7 were calculated as shown in Fig. 14. It was found that the decorrelation time (i.e., the temporal lag at which the autocorrelation coefficient drops to 1/*e*, where $e \approx 2.72$) was approximately 1 day for all three datasets. As the temporal lag increased, the three autocorrelation coefficients initially decreased notably and then reduced only slightly. This indicates that both types of satellite data showed similar key features to the RG observations. The key features of the autocorrelation coefficients for CMORPH and TRMM-3B42v7 indicate that both types of satellite data were stationary (Yu et al., 2007) and displayed weak dependence on themselves. Therefore, from the perspective of dependency on the data itself, both types of satellite data performed well (Chokngamwong and Chiu 2008).

To further examine the performances of the two types of satellite data, we conducted a trend comparison as follows. First, the linear trends of annual accumulated precipitation at each of the 91 available stations (Fig. 1) during the 15-yr period were calculated for RG, CMORPH, and TRMM-3B42v7. The Student's *t* test (Huang 1999) shows that only 13% of the trends (at 91 stations) can reach the significance level of 90%. For Thailand as a whole, the mean linear trends for RG, CMORPH, and TRMM-3B42v7 were 5.72, 2.25, and 4.54 mm year^{-1}, respectively. These values indicate that annual precipitation over Thailand increased during the 15-yr period. To further evaluated the precipitation variation within different regions, using Eqs. (1–3), the BIAS, RMSD, and MAD values were calculated for the trends of each type of satellite precipitation data relative to the trend of the RG observations. The results are presented in Table 5. BIAS shows that TRMM-3B42v7 and CMORPH both underestimate the 15-yr linear trend in the whole and Northeast Thailand, whereas, in other regions, if TRMM-3B42v7 shows an overestimation, CMORPH will show an underestimation, and vice versa. Overall, TRMM-3B42v7 is better than CMORPH (because the absolute values of BIAS, RMSD and MAD are smaller for the TRMM-3B42v7 precipitation data), except for South Thailand.

7. Conclusion and Discussion

Based on a detailed evaluation during a 15-yr period, this study filled in the deficiencies of current evaluations of TRMM-3B42v7's performances in Thailand, conducted the first evaluation of CMORPH in this region, and contrasted the relative performances of these two datasets. We strongly suggest that, prior to analyzing specific features of the precipitation over Thailand by using satellite data, readers review the information presented in Tables 6 and 7. These two tables reveal the actual abilities of CMORPH and TRMM-3B42v7 to reproduce specific precipitation features. If a satellite data can reproduce a specific feature of precipitation credibly, this data can be used to as a supplement for the real precipitation observation, otherwise, we suggest researchers to use RG-observed precipitation data. Appropriate selection of precipitation data will improve the reliability of research results.

For Thailand as a whole, only 12 of the 35 factors listed in Table 6 could be reproduced credibly by the two types of satellite data (11 for CMORPH and 10 for TRMM-3B42v7). Both TRMM-3B42v7 and CMORPH displayed notable limitations in reproducing the intensity and spatial distribution pattern of extreme precipitation. Detailed comparisons indicated that TRMM-3B42v7 exhibited better performances than CMORPH for 22 of the 35 factors (Table 6), showed similar performances to CMORPH for 7 factors, and displayed worse performances than CMORPH for only 6 factors. Overall, these results demonstrate that, for Thailand as a whole, TRMM-3B42v7 is superior to CMORPH in representing real precipitation. Detection sensors and precipitation retrieval algorithms differed from each other notably for TRMM-3B42v7 and CMORPH precipitation data (Table 8). This is the most important reason for the different performances of them. Other factors such as geographical features, quality of the RG observed precipitation and the interpolating-grid-points-into-stations evaluation manner (particularly for those associated with rainfall intensity such as non-precipitation days, CRR, RMSD, MAD, RE, etc.) can also affect the performances of satellite data (Shen et al., 2010; Cheng et al., 2014; Arshad et al. 2020; Chua et al. 2020).

In each region of Thailand, 9, 8, 8, 7, and 7 of the 19 factors listed in Table 7 were reproduced credibly for North, Northeast, Central, East, and South Thailand, respectively. CRR of the dry season and interval/duration of rainfall events during the rainy season could not be credibly reproduced for any of the regions. Comparisons showed that in North and

Northeast Thailand, TRMM-3B42v7 was found to be superior to CMORPH as 13 of the 19 factors were better. For East and South Thailand, TRMM-3B42v7 also exhibited superior performances to CMORPH, as 15 of the 19 factors were better. Central Thailand was the only region where CMORPH (8 factors were better) displayed a similar performance to TRMM-3B42v7 (9 factors were better). If only intensity is considered, CMORPH (7 factors were better) was superior to TRMM-3B42v7 (4 factors were better) for Central Thailand.

As Chokngamwong and Chiu (2008) conducted a research on the similar topic over Thailand, we compared this study to theirs and found that there were five aspects need to be noted: (i) for the CDF of rain rate over entire Thailand, version 7 of TRMM-3B42v7 data showed a lower rainfall probability than those of versions 5-6, and its performance was better than that of CMORPH. (ii) For the monthly precipitation in different regions of Thailand, although similar variation features were found by versions 5-7 of TRMM-3B42v7 and CMORPH data, relative errors were the smallest for version 7 of TRMM-3B42v7 data, implying its performance was the best. (iii) For the duration and interval of rainfall events, versions 6-7 of TRMM-3B42v7 data made credible estimations of real rainfall interval in different regions of Thailand, particularly for the rainy season. Compared to CMORPH, version 7 of TRMM 3B42 data showed an overall better performance. (iv) For BIAS, RMSD, and MAD over different regions of Thailand, version 6 of TRMM 3B42 data mainly showed smaller values than those of version 5, which means its performance was better. Version 7 of TRMM 3B42 data showed a better performance than CMORPH in terms of BIAS, whereas, CMORPH was better in terms of MAD and RMSD. Version 6 of TRMM 3B42 data showed a better performance than version 7 in terms of BIAS over all regions except for Northeast and

East Thailand; in terms of RMSD, version 7 was better except for North and Central Thailand; and in terms of MAD, version 7 was better in all regions. (v) For the dataset autocorrelation over entire Thailand, versions 5-7 of TRMM 3B42 and CMORPH precipitation data all showed a low autocorrelation, implying that they all displayed a weak dependence on themselves.

Compared to previous studies on the similar topic other than Thailand, new findings are as follows: (i) Shen et al. (2010) found that CMORPH was better than TRMM-3B42v6 in representing the spatial pattern of precipitation over China, whereas, this study found that TRMM-3B42v7 was better for Thailand in this aspect. (ii) Luo et al. (2013) found that CMORPH notably overestimated the non-precipitation days' proportion in the Yangtze-Huai River Basin, whereas this study found that CMORPH made a notable underestimation in this aspect for Thailand. (iii) Chua et al. (2020) evaluated the performance of CMORPH in representing rain/no-rain events in Australia and found that CMORPH showed a good performance. In contrast, this study found that rain events' proportion was notably overestimated by CMORPH in Thailand. (iv) Arshad et al. (2020) found that TRMM-3B42RTv7 was able to capture the extreme precipitation events in Pakistan, whereas, this study found TRMM-3B42v7 showed a lower probability of detection of extreme rainfall events over Thailand.

Acknowledgments

The authors thank NASA (National Aeronautics and Space Administration), the NOAA (National Oceanic and Atmospheric Administration), and the TMD (Thailand Meteorological

Department) for providing the data. This research was supported by the National Key R&D Program of China (grant number 2018YFC0809400), the National Natural Science Foundation of China (grant numbers 41861144015 and 41775046), and the Youth Innovation Promotion Association of the Chinese Academy of Sciences.

References

Arshad, M., and Coauthors, 2020. Evaluation of GPM-IMERG and TRMM-3B42 precipitation products over Pakistan. *Atmospheric Research*, **249**, doi: 10.1016/j.atmosres.2020.105341.

Babaousmail, H., Hou, R. T., Ayugi, B., and Gnitou, G. T., 2019. Evaluation of satellite-based precipitation estimates over Algeria during 1998-2016. *J. Atmos. Solar-Terr. Phys.*, **195**, doi: 10.1016/j.jastp.2019.105139.

Belete, M., Deng, J. S., Wang, K., Zhou, M. M., Zhu, E. Y., Shifaw, E., and Bayissa, Y., 2020. Evaluation of satellite rainfall products for modeling water yield over the source region of Blue Nile Basin. *Science of the Total Environment*, **708**, 134834, doi: 10.1016/j.scitotenv.2019.134834.

Chen S., Hong Y., and Coauthors, 2013. Evaluation of the successive V6 and V7 TRMM multisatellite precipitation analysis over the Continental United States. *Water Resources Research*, **49**, 8174-8186, doi: 10.1002/2012WR012795.

Cheng, L., Shen, R. P., Shi, C. X., Bai, L., and Yang, Y. H.,2014. Evaluation and Verification of CMORPH and TRMM 3B42 Precipitation Estimation Products. *Meteorological Monthly*, **40**, 1372-1379, doi: 10.7519/j.issn.1000-0526.2014. 11.010.

Cheong, W. K., Timbal, B., Golding, N., Sirabaha, S., Kwan, K.F., Cinco, T. A., Archevarahuprok, B., Vo, VH., Gunawan, D., and Han, S., 2018. Observed and modelled temperature and precipitation extremes over Southeast Asia from 1972 to 2010. *Int. J. Climatol.*, **38**, 3013-3027, doi: 10.1002/joc.5479.

Chokngamwong, R., and Chiu, L. S., 2008. Thailand daily rainfall and comparison with TRMM products. *J. Hydrometeor.*, **9**, 256-266, doi: 10.1175/2007JHM876.1.

Chua, Z. W., Kuleshov, Y., and Watkins, A., 2020. Evaluation of Satellite Precipitation Estimates over Australia. *Remote Sensing*, **12**, doi: 10.3390/rs12040678.

Ding Y. H., Si D., Liu Y. J., Wang Z. Y., Li Y., Zhao L., and Song Y. F., 2018. On the Characteristics, Driving Forces and Inter-decadal Variability of the East Asian Summer Monsoon. *Chinese J. Atmos. Sci.*, **42**, 533-558, doi: CNKI:SUN:DQXK.0.2018-03-006.

Huang, J. Y., 1999. Statistic analysis and forecast methods in meteorology (in Chinese). Beijing: China Meteorological Press.

Huang, A. M., Zhao, Y., Zhou, Y., Yang, B., Zhang, L. J., Dong, X. N., Fang, D. X., and Wu, Y., 2016. Evaluation of multisatellite precipitation products by use of ground-based data over China. *J. Geophys. Res-atmos.*, **121**, 10654-10675, doi: 10.1002/2016JD025456.

Huffman, G. J., D. T. Bolvin, E. J. Nelkin, D. B. Wolff, R. F. Adler, G. Gu, Y. Hong, K. P. Bowman, and E. F. Stocker, 2007. The TRMM Multisatellite Precipitation Analysis (TMPA): Quasi-global, multiyear, combined-sensor precipitation estimates at fine scales. *J. Hydrometeor.*, **8**, 38–55, doi: 10.1175/jhm560.1.

IPCC 2014, *Summary for Policymakers. Climate Change 2014: Impacts, Adaptation and Vulnerability. Contribution of Working Group II to the Fifth Assessment Report of the Intergovernmental Panel on Climate Change*, https://ipcc-wg2.gov/AR5/

John, A., 2013. Price relations between export and domestic rice markets in Thailand. *Food Policy*, **42**, 48-57, doi: 10.1016/j.foodpol.2013.06.001.

Joyce, R. J., J. E. Janowiak, P. A. Arkin, and P. Xie, 2004. CMORPH: A method that produces global precipitation estimates from passive microwave and infrared data at high spatial and temporal resolution. *J. Hydrometeorol.*, **5**, 487–503, doi: 10.1175/1525-7541(2004)005<0487:Camtpg>2.0.Co;2.

Kidd, C., P. Bauer, J. Turk, G. J. Huffman, R. Joyce, K.-L. Hsu, and D. Braithwaite, 2012. Intercomparison of high-resolution precipitation products over northwest Europe. *J. Hydrometeorol.*, **13**, 67–83, doi: 10.1175/JHM-D-11-042.1.

Kim, I. W., Oh, J., Woo, S., and Kripalani, R. H., 2019. Evaluation of precipitation extremes over the Asian domain: observation and modelling studies. *Climate Dynamics*, **52**, 1317-1342, doi: 10.1007/s00382-018-4193-4.

Kolmogorov, A. N., 1933. Sulla determinazione empirica di una legge di distribuzione. Giornale dell'Istituto Italiano degli Attuari, **4**, 83–91.

Li R., Shi J. C., Ji D. B., Zhao, T. J., Plermkamon, V., Moukomla, S., Kuntiyawichai, K., and Kruasilp, J., 2019. Evaluation and Hydrological Application of TRMM and GPM Precipitation Products in a Tropical Monsoon Basin of Thailand. *Water*, **11**, 818, doi: 10.3390/w11040818.

Luo, Y. L., Qian, W., Zhang, R., and Zhang, D. L., 2013. Gridded hourly precipitation analysis from high-density rain gauge network over the yangtze-huai rivers basin during the 2007 mei-yu season and comparison with cmorph. *Journal of Hydrometeorology*, **14**, 1243-1258, doi: 10.1175/JHM-D-12-0133.1.

Manomaiphiboon, K., Octaviani, M., Torsri, K., and Towprayoon, S., 2013. Projected changes in means and extremes of temperature and precipitation over thailand under three future emissions scenarios. *Climate Research*, **58**, 97-115, doi: 10.3354/cr01188.

Mastylo, M.,2013. Bilinear interpolation theorems and applications. *Journal of Functional Analysis*, **265**, 185-207, doi: 10.1016/j.jfa.2013.05.001.

Morrissey, M. L., J. A. Maliekal, J. S. Greene, and J. Wang, 1995. The uncertainty of simple spatial averages using rain gauge networks. *Water Resour. Res.*, **31**, 2011–2017, doi: 10.1029/95WR01232.

Nair, S., G. Srinivasan, and R. Nemani, 2009. Evaluation of multi-satellite TRMM derived rainfall estimates over a Western State of India. *J. Meteorol. Soc. Jpn.*, **87**, 927–939, doi: 10.2151/jmsj.87.927.

Promchote, P., Simon Wang, S. Y., and Johnson, P. G., 2016. The 2011 great flood in Thailand: climate diagnostics and implications from climate change. *J. Clim.*, **29**, 367-379, doi: 10.1175/JCLI-D-15-0310.1.

Schaefer, J. T., 1990. The critical success index as an indicator of warning skill. *Wea. Forecasting*, **5**, 570-575.

Schulz, J., Albert, P., and Coauthors, 2009. Operational climate monitoring from space: The EUMETSAT Satellite Application Facility on Climate Monitoring (CM-SAF). *Atmos. Chem. Phys.*, **9**, 1687–1709, doi: 10.5194/acp-9-1687-2009.

Sekaranom, A. B., and Masunaga, H., 2018. Origins of heavy precipitation biases in the TRMM PR and TMI products assessed with cloudsat and reanalysis data. *Journal of Applied Meteorology and Climatology*, **58**, doi: 10.1175/JAMC-D-18-0011.1.

Shen, Y., A. Xiong, Y. Wang, and P. Xie, 2010: Performance of high-resolution satellite precipitation products over China. *J. Geophys. Res.*, **115**, 2114, doi: 10.1029/2009JD012097.

Smirnov, N., 1948. Table for Estimating the Goodness of Fit of Empirical Distributions. *Annals of Mathematical Statistics*, **19**, 279-281, doi: 10.1214/aoms/1177730256.

Soo, E. Z. X., Jaafar, W. Z. W., Lai, S. H., Othman, F., Elshafie, A., Islam, T., Srivastava, P., Hadi, H. S. O., 2020. Evaluation of bias-adjusted satellite precipitation estimations for extreme flood events in Langat river basin, Malaysia. *Hydrol. Res.*, **51**, 105-126, doi: 10.2166/nh.2019.071.

Tangang, F., and Coauthors, 2019. Projected future changes in mean precipitation over Thailand based on multi-model regional climate simulations of CORDEX Southeast Asia. *Int. J. Climatol.*, **39**, 5413-5436, doi: 10.1002/joc.6163.

Torsri, K., Octaviani, M., Manomaiphiboon, and K., Towprayoon, S., 2013. Regional mean and variability characteristics of temperature and precipitation over thailand in 1961-2000 by a regional climate model and their evaluation. *Theoretical & Applied Climatology*, **113**, 289-304, doi: 10.1007/s00704-012-0782-z.

Veerakachen, W., Raksapatcharawong, M., Seto, S., 2014. Performance evaluation of Global Satellite Mapping of Precipitation (GSMaP) products over the Chaophraya River basin, Thailand. *Hydrological Research Letters*, **8**, 39-44. doi: 10.3178/hrl.8.39.

Villanueva, O. M. B., ZambranoBigiarini, M., Ribbe, L., Nauditt, A., Giraldo-Osorio, J. D., and Thinh, N. X., 2018. Temporal and spatial evaluation of satellite rainfall estimates over different regions in Latin-America. *Atmos. Res.*, **213**, 34-50, doi: 10.1016/j.atmosres.2018.05.011.

Xu, R., Tian, F. Q., Yang, L., Hu, H. C., Lu, H., and Hou, A. Z., 2017. Ground validation of GPM IMERG and TRMM 3B42V7 rainfall products over southern Tibetan Plateau based on a high-density rain gauge network. *J. Geophys. Res-atmos.*, **122**, 910-924, doi: 10.1002/2016JD025418.

Yang, Y. F., Wu, J., Bai, L., and Wang, B, 2020. Reliability of Gridded Precipitation Products in the Yellow River Basin, China. *Remote Sensing*, **12**, doi: 10.3390/rs12030374.

Yu N. L., Yi D. Y., and Tu X. Q., 2007. Analysis of auto-correlations and partial-correlation functions in time series. *Mathematical Theory and Applications*, **27**, 54−57.

Table captions

Table 1. Indication of variables in skill measures (probability of detection (POD), false alarm rate (FAR), and critical success index (CSI)) (Schaefer 1990).

Table 2. Mean daily precipitation intensity (DPI; accumulated precipitation divided by the total number of days during the 15-yr period, mm day^{-1}), conditional rain rate (CRR; averaged daily precipitation intensity for all rainfall days, mm day^{-1}), and the precipitation day fraction (PDF; number of rainfall days divided by the total number of days) for the five regions of Thailand during the 15-yr period. NE=Northeast; RG=rain gauge; C=CMORPH; T=TRMM-3B42v7. The values showing better performance of the satellite data are indicated in bold type.

Table 3. Bias (BIAS), root-mean-square difference (RMSD), and mean absolute difference (MAD) for CMORPH (values outside parentheses) and TRMM-3B42v7 (values inside parentheses) for all regions of Thailand from 1998 to 2012 (mm day^{-1}). For each of the 91 stations throughout Thailand, its BIAS, MAD, and RMSD values during the 15-yr period were first calculated using the satellite data, and then these three parameters were spatially averaged for each region. RG=rain gauge. The values showing better performance of the satellite data are indicated in bold type.

Table 4. Probability of detection (POD), false alarm rate (FAR), and critical success index (CSI) for CMORPH (values outside parentheses) and TRMM-3B42v7 (values inside

parentheses) over Thailand as a whole during different seasons of the 15-yr period. DJF=December, January, February; MAM=March, April, May; JJA=June, July, August; SON=September, October, November. The values showing better performance of the satellite data are indicated in bold type.

Table 5. Bias (BIAS), root-mean-square difference (RMSD), and mean absolute difference (MAD) for the linear trends of CMORPH (values outside parentheses) and TRMM-3B42v7 (values inside parentheses) over the 15-yr period within different regions. Better performances of the satellite data are highlighted by bold.

Table 6. Comparisons between TRMM-3B42v7 and CMORPH for Thailand as a whole, where "O" represents overestimate, "U" represents underestimate, "*" indicates the data with better performance, "S" indicates that both sets of data displayed similar performance, and "--" means none. "/" indicates that the data is quantitatively credible, i.e., a relative error of less than 20%. DPI=daily precipitation intensity, CRR=conditional rain rate, PDF=precipitation day fraction (the number of precipitation days divided by the total number of days), RMSD=root-mean-square difference, MAD=mean absolute difference, RE=relative error, FAR=false alarm rate, POD=probability of detection, CSI=critical success index, CTV=characteristics of temporal variation, CDF=cumulative distribution function, NPD=non-precipitation days, DTM=daily to monthly, EY=entire year, DS=dry season, RS=rainy season.

Table 7. Comparisons between TRMM-3B42v7 and CMORPH for each of five regions of Thailand, where "O" represents overestimate, "U" represents underestimate, "*" indicates the data with better performance, "S" indicates that both sets of data displayed similar performance, and "--" means none. "/" indicates that the data is quantitatively credible, i.e., a relative error of less than 20%. C=CMORPH, T=TRMM-3B42v7, NE=northeast, DPI=daily precipitation intensity, CRR=conditional rain rate, PDF=precipitation day fraction (the number of precipitation days divided by the total number of days), RMSD=root-mean-square difference, MAD=mean absolute difference, RE=relative error, CTV=characteristics of temporal variation, EY=entire year, DS=dry season, RS=rainy season.

Table 8. Contrasts of the four types of satellite precipitation products.

Figure captions

Figure 1. Geographical distributions of the 15-yr averaged annual precipitation in Thailand. The shading indicates the terrain characteristics (units: m). "n" indicates the number of stations in different regions.

Figure 2. Annual (accumulated) precipitation (CMORPH, TRMM-3B42v7, and RG; mm) for the various regions: (a) whole of Thailand, (b) Central Thailand, (c) North Thailand, (d) South Thailand, (e) Northeast Thailand, and (f) East Thailand. RG=rain gauge, CC=correlation coefficient.

Figure 3. Relative errors of the annual CMORPH and TRMM-3B42v7 precipitation (%) for the various regions: (a) whole of Thailand, (b) Central Thailand, (c) North Thailand, (d) South Thailand, (e) Northeast Thailand, and (f) East Thailand.

Figure 4. 15-yr averaged monthly (accumulated) precipitation (CMORPH, TRMM-3B42v7, and RG; mm) for the various regions: (a) whole of Thailand, (b) Central Thailand, (c) North Thailand, (d) South Thailand, (e) Northeast Thailand, and (f) East Thailand. RG=rain gauge, CC=correlation coefficient.

Figure 5. Relative errors of the 15-yr averaged monthly CMORPH and TRMM-3B42v7 precipitation (%) for the various regions: (a) whole of Thailand, (b) Central Thailand, (c) North Thailand, (d) South Thailand, (e) Northeast Thailand, and (f) East Thailand.

Figure 6. (a) RG-based mean conditional rain rate (CRR; mm day^{-1}) of precipitation events for various regions during different periods. (b) and (c) Ratio of the CRR for CMORPH and TRMM-3B42v7 to that for RG, respectively (%). RG=rain gauge, A=all regions, N=North Thailand, NE=Northeast Thailand, C=Central Thailand, E=East Thailand, S=South Thailand.

Figure 7. Cumulative distribution functions of the daily precipitation at the 91 stations during the 15-yr period (498,589 samples for each dataset) derived from the RG, CMORPH, and TRMM-3B42v7 data, where the three solid black lines divide the precipitation into four

categories (i.e., light to none, moderate, heavy, and torrential rainfall) according to intensity. The proportions of the four precipitation categories for three types of precipitation data are indicated in different colors, where green represents RG, blue represents CMORPH, and red represents TRMM-3B42v7. RG=rain gauge.

Figure 8. Boxplot of the ratio of the satellite data to RG-observed data for extreme precipitation (first 5% in the ranking of precipitation intensity based on total samples of 91 stations). The boxes indicate the 25th (Q1) to 75th (Q3) percentiles and the red line indicates the median value. The whiskers indicate the range of [Q1−1.5×(Q3−Q1)] or the minimum of the data (if all values in the data are bigger than the value calculated by the above expression) and [Q3+1.5×(Q3−Q1)] or the maximum of the data (if all values in the data are smaller than the value calculated by the above expression). RG=rain gauge.

Figure 9. Linear correlation coefficients between the running means (the days used for the running means are indicated in the abscissa) of the RG and satellite precipitation data (CMORPH/TRMM-3B42v7). RG=rain gauge.

Figure 10. Boxplot of the spatial correlation between the satellite data (CMORPH/TRMM-3B42v7) and RG observations during the 15-yr period. The boxes indicate the 25th (Q1) to 75th (Q3) percentiles and the red line indicates the median value. The whiskers indicate the range of [Q1−1.5×(Q3−Q1)] or the minimum of the data (if all values in the data are bigger than the value calculated by the above expression) and

[Q3+1.5×(Q3−Q1)] or the maximum of the data (if all values in the data are smaller than the value calculated by the above expression). RG=rain gauge.

Figure 11. Critical success index (CSI) for CMORPH and TRMM-3B42v7 as a function of the number of days used for the running mean (abscissa).

Figure 12. Probability of detection (POD), false alarm rate (FAR), and critical success index (CSI) for CMORPH and TRMM-3B42v7 relative to the rainfall intensity (the values in the abscissa indicate that the POD, FAR, and CSI values were calculated using rainfall intensities above that value) during the 15-yr period for the whole of Thailand.

Figure 13. (a) RG-based mean precipitation interval (days) and (b) duration (days) for precipitation events in the various regions during different periods. (c) and (d) Ratio of the mean interval and duration for CMORPH to those for RG, respectively (%). (e) and (f) Ratio of the mean interval and duration for TRMM-3B42v7 to those for RG, respectively (%). The red dotted horizontal line is at 100%. RG=rain gauge, A=all regions, N=North Thailand, NE=Northeast Thailand, C=Central Thailand, E=East Thailand, S=South Thailand.

Figure 14. Temporal autocorrelation coefficients for RG, CMORPH, and TRMM-3B42v7. RG=rain gauge.

Table 1. Explanation of variables in skill measures (probability of detection (POD), false alarm rate (FAR), and critical success index (CSI)) (Schaefer 1990).

		Surface observation	
		precipitation	no precipitation
Satellite data	precipitation	V_a	V_c
	no precipitation	V_b	V_d

Table 2. Mean daily precipitation intensity (DPI; accumulated precipitation divided by the total number of days during the 15-yr period, mm day^{-1}), conditional rain rate (CRR; averaged daily precipitation intensity for all rainfall days, mm day^{-1}), and the precipitation day fraction (PDF; number of rainfall days divided by the total number of days) for the five regions of Thailand during the 15-yr period. NE=Northeast; RG=rain gauge; C=CMORPH; T=TRMM-3B42v7. The values showing better performance of the satellite data are indicated in bold type.

		Whole	North	NE	Center	East	South
15-yr	RG	4.47	3.60	4.03	3.53	6.13	6.84
mean	C	4.11	3.28	3.63	**3.73**	5.05	6.10
DPI	T	**4.62**	**3.84**	**4.36**	4.14	**5.54**	**6.41**
15-yr	RG	12.02	10.66	12.44	10.68	14.43	14.26
mean	C	6.97	6.20	7.34	6.53	7.60	8.06
CRR	T	**8.81**	**7.70**	**9.37**	**8.30**	**9.51**	**10.25**
15-yr	RG	0.36	0.34	0.32	0.33	0.39	0.48
mean	C	0.58	0.53	0.50	0.58	0.65	0.76
PDF	T	**0.52**	**0.50**	**0.47**	**0.50**	**0.57**	**0.63**

Table 3. Bias (BIAS), root-mean-square difference (RMSD), and mean absolute difference (MAD) for CMORPH (values outside parentheses) and TRMM-3B42v7 (values inside parentheses) for all regions of Thailand from 1998 to 2012 (mm day^{-1}). For each of the 91 stations throughout Thailand, its BIAS, MAD, and RMSD values during the 15-yr period were first calculated using the satellite data, and then these three parameters were spatially averaged for each region. RG=rain gauge. The values showing better performance of the satellite data are indicated in bold type.

	Whole	North	Northeast	Center	East	South
BIAS	-0.36	-0.32	-0.40	**0.21**	-1.09	-0.74
	(**0.15**)	(**0.25**)	(**0.33**)	(0.62)	(**-0.59**)	(**-0.43**)
MAD	**4.24**	**3.49**	**3.78**	**3.84**	**5.44**	**6.01**
	(4.49)	(3.74)	(4.02)	(4.07)	(5.82)	(6.21)
RMSD	**10.53**	**8.97**	**10.18**	**9.60**	**13.06**	**13.50**
	(10.74)	(9.11)	(10.25)	(9.93)	(13.59)	(13.69)

Table 4. Probability of detection (POD), false alarm rate (FAR), and critical success index (CSI) for CMORPH (values outside parentheses) and TRMM-3B42v7 (values inside parentheses) over Thailand as a whole during different seasons of the 15-yr period. DJF=December, January, February; MAM=March, April, May; JJA=June, July, August; SON=September, October, November. The values showing better performance of the satellite data are indicated in bold type.

	Entire year	DJF	MAM	JJA	SON
POD	**0.93** (0.88)	**0.72** (0.64)	**0.94** (0.91)	**0.96** (0.91)	**0.94** (0.89)
FAR	0.42 (**0.39**)	0.65 (**0.62**)	0.44 (**0.40**)	0.37 (**0.33**)	0.35 (**0.32**)
CSI	0.55 (**0.57**)	0.31 (0.31)	0.54 (**0.56**)	0.61 (**0.62**)	0.62 (**0.63**)

Table 5. Bias (BIAS), root-mean-square difference (RMSD), and mean absolute difference (MAD) for the linear trends of CMORPH (values outside parentheses) and TRMM-3B42v7 (values inside parentheses) over the 15-yr period within different regions. Better performances of the satellite data are highlighted by bold.

	Whole	North	Northeast	Center	East	South
BIAS	-3.46	-6.46	-8.12	-4.34	11	**1.28**
	(**-1.17**)	(**1.64**)	(**-5.41**)	(**2.00**)	(**-2.02**)	(-4.17)
MAD	12.88	10.92	12.69	14.9	16.04	12.35
	(**9.68**)	(**8.31**)	(**9.44**)	(**10.65**)	(**8.01**)	(**11.90**)
RMSD	16.58	14.89	15.3	18.88	18.56	16.71
	(**12.77**)	(**10.94**)	(**12.30**)	(**13.92**)	(**10.00**)	(**15.62**)

Table 6. Comparisons between TRMM-3B42v7 and CMORPH for Thailand as a whole, where "O" represents overestimate, "U" represents underestimate, "*" indicates the data with better performance, "S" indicates that both sets of data displayed similar performance, and "--" means none. "/" indicates that the data is quantitatively credible, i.e., a relative error of less than 20%. DPI=daily precipitation intensity, CRR=conditional rain rate, PDF=precipitation day fraction (the number of precipitation days divided by the total number of days), RMSD=root-mean-square difference, MAD=mean absolute difference, RE=relative error, FAR=false alarm rate, POD=probability of detection, CSI=critical success index, CTV=characteristics of temporal variation, CDF=cumulative distribution function, NPD=non-precipitation days, DTM=daily to monthly, EY=entire year, DS=dry season, RS=rainy season.

Evaluation factors				CMORPH	TRMM-3B42v7
Intensity	Overall features	DPI		U/	O*/
		CRR		U	U*
		PDF		O	O*
		BIAS		--	*
		MAD		*	--
		RMSD		*	--
	Annual	CTV		S/	
		RE		U/	O*/
	Monthly	CTV		S/	
		RE	DS	U/	U*/
			RS	U/	O*/
	DS	CRR		U	U*
	RS	CRR		U	U*/
	Daily (CDF)	NPD, small, and heavy rainfall		--/	*/
		torrential rainfall		--	*
		Moderate rainfall		*/	--
	Extreme rainfall			--	*
	Correlation of rain rate of different temporal scales			--/	*/

Table 6 (Continued)

Evaluation factors				CMORPH	TRMM-3B42v7
Spatial distribution pattern	Overall features	POD		*	--
		FAR		--	*
		CSI		--	*
		Spatial correlation		S	
	Different temporal scales	Seasonal (especially from Mar to Nov)	POD	*	--
			FAR	--	*
			CSI	--	*
		DTM	CSI	S	
	Different precipitation intensity (POD, FAR, and CSI)			--	*
Interval	EY			U*/	U
	RS			U	U*
	DS			S (U)	
Duration	EY			O	O*
	RS			O	O*
	DS			S (O)	
Auto-Correlation and 15-yr trend	Temporal autocorrelation			S/	
	15-yr precipitation linear trend			--	*

Table 7. Comparisons between TRMM-3B42v7 and CMORPH for each of five regions of Thailand, where "O" represents overestimate, "U" represents underestimate, "*" indicates the data with better performance, "S" indicates that both sets of data displayed similar performance, and "--" means none. "/" indicates that the data is quantitatively credible, i.e., a relative error of less than 20%. C=CMORPH, T=TRMM-3B42v7, NE=northeast, DPI=daily precipitation intensity, CRR=conditional rain rate, PDF=precipitation day fraction (the number of precipitation days divided by the total number of days), RMSD=root-mean-square difference, MAD=mean absolute difference, RE=relative error, CTV=characteristics of temporal variation, EY=entire year, DS=dry season, RS=rainy season.

Evaluation methods			Regions									
			North		NE		Central		East		South	
			C	T	C	T	C	T	C	T	C	T
Intensity	Overall features	DPI	U/	O*/	U/	O*/	O*/	O/	U/	U*/	U/	U*/
		CRR	U	U*/	U	U*	U	U*	U	U*	U	U*
		PDF	O	O*	O	O*	O	O*	O	O*	O	O*
		BIAS	--	*	--	*	*	--	--	*	--	*
		MAD	*	--	*	--	*	--	*	--	*	--
		RMSD	*	--	*	--	*	--	*	--	*	--
	Annual	CTV	S/		S/		S/		--	*/	S/	
		RE	U/	O*/	U/	O*/	O*/	O/	U/	U*/	U	U*/
	Monthly	CTV	S/		S/		S/		S/		S/	
		RE DS	U/	U*/	U/	U*/	U*/	U	U*/	U/	U/	U*/
		RE RS	U/	O*/	U/	O*/	O*/	O/	U/	U*/	U/	U*/
	DS	CRR	U	U*	U	U*	U	U*	U	U*	U	U*
	RS	CRR	U	U*/	U	U*/	U	U*/	U	U*	U	U*
Interval		EY	U*/	U/	U*/	U	U*	U	U	U*	U	U*
		RS	U	U*	U	U*	U	U*	U	U*	U	U*
		DS	U*	U	U*	U	U	U*	U	U*	U	U*
Duration		EY	O	O*	O	O*	O	O*	O	O*	O	O*
		RS	O	O*	O	O*	O	O*	O	O*	O	O*
		DS	O	O*	O	O*	O	O*/	O	O*/	O	O*/

Table 8. Contrasts of the four types of satellite precipitation products.

<table>
<tr><th></th><th>TRMM 3B42 version 5</th><th>TRMM 3B42 version 6</th><th>TRMM 3B42 version 7</th><th>CMORPH</th></tr>
<tr><td>Sensors</td><td colspan="3">Precipitation Radar (PR)
TRMM Microwave Imager (TMI)
Visible and Infrared (IR) Scanner</td><td>IR brightness temperature detector
Passive microwave detector</td></tr>
<tr><td>Algorithms</td><td colspan="3">3B42 algorithm:
(1) The microwave precipitation estimates are calibrated and combined.
(2) IR precipitation estimates are created using the calibrated microwave precipitation.
(3) The microwave and IR estimates are combined.
(4) Rescaling to monthly data is applied.</td><td>Morphing technology:
(1) Calculate the motion vector of the precipitation cloud system according to the IR brightness temperature data observed by geostationary satellite.
(2) Extrapolate the instantaneous precipitation distribution obtained from passive microwave inversion of low-orbit satellites to the target time along the motion vector to obtain the spatial continuous precipitation distribution.</td></tr>
<tr><td rowspan="2">Algorithm differences</td><td rowspan="2">An IR estimated rain rate from calibrate IR estimates from geosynchronous satellite IR data calibrated to TRMM Combined Instrument (TCI).</td><td colspan="2">(1) High-quality TRMM data are combined with high-quality passive-microwave-based rain estimates from orbiting satellites, which are calibrated by TRMM PR/TMI.
(2) Merged with gauge measurements.</td><td rowspan="2">A blending technique, rather than a precipitation algorithmic estimation procedure.</td></tr>
<tr><td>none</td><td>Incorporates more satellite observations and uses a more recent gauge analysis from the Global Precipitation Climatology Centre.</td></tr>
</table>

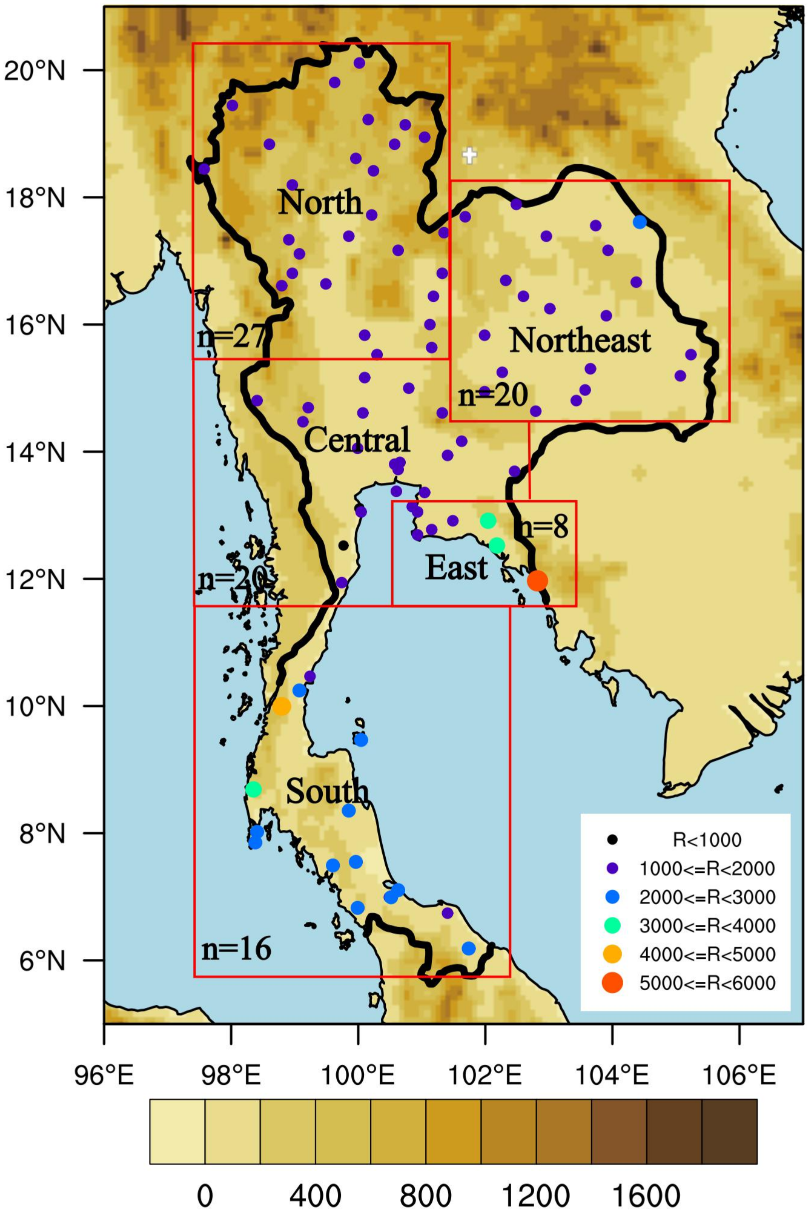

Figure 1. Geographical distributions of the 15-yr averaged annual precipitation in Thailand. The shading indicates the terrain characteristics (units: m). “n” indicates the number of stations in different regions.

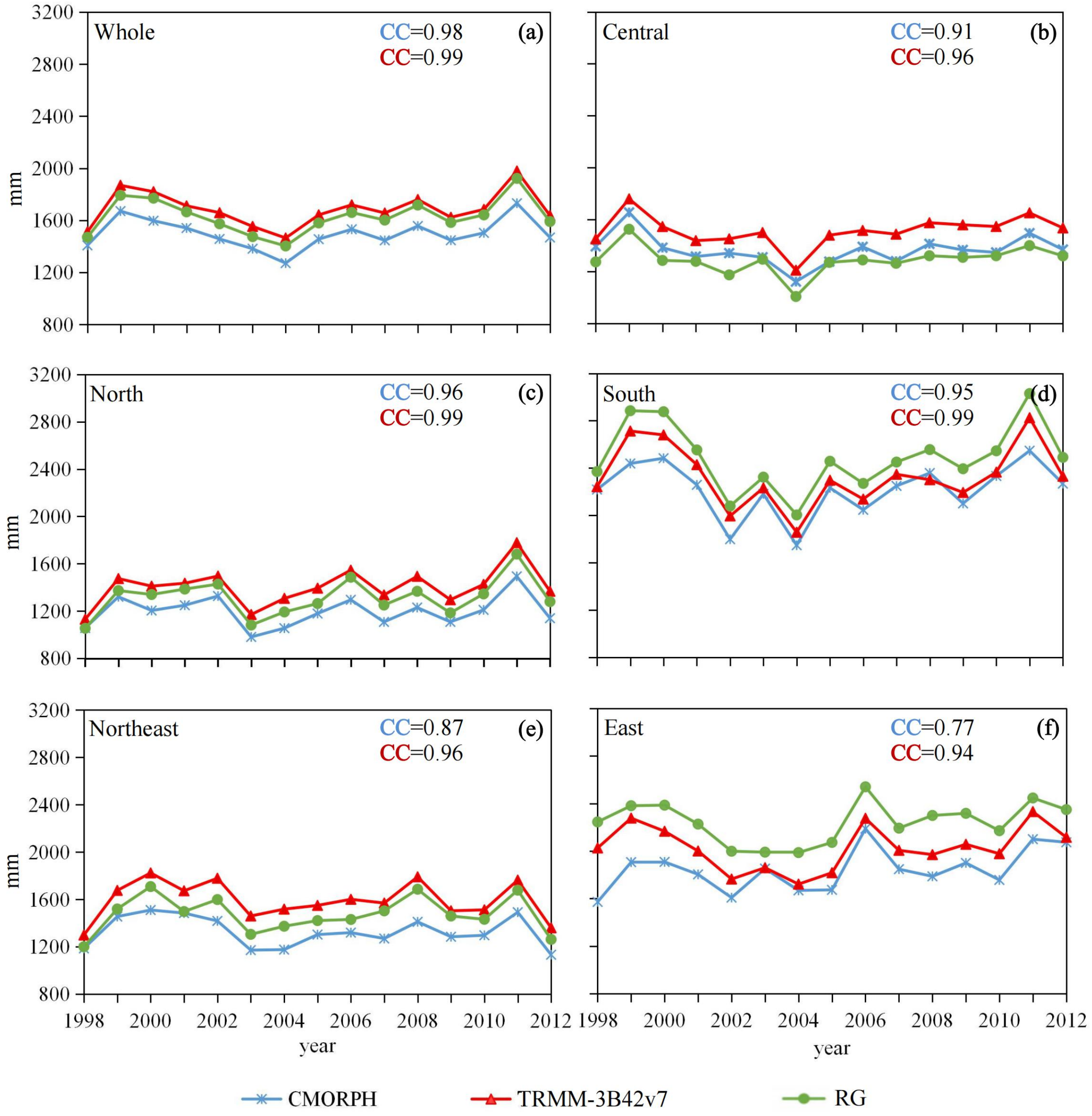

Figure 2. Annual (accumulated) precipitation (CMORPH, TRMM-3B42v7, and RG; mm) for the various regions: (a) whole of Thailand, (b) Central Thailand, (c) North Thailand, (d) South Thailand, (e) Northeast Thailand, and (f) East Thailand. RG=rain gauge, CC=correlation coefficient.

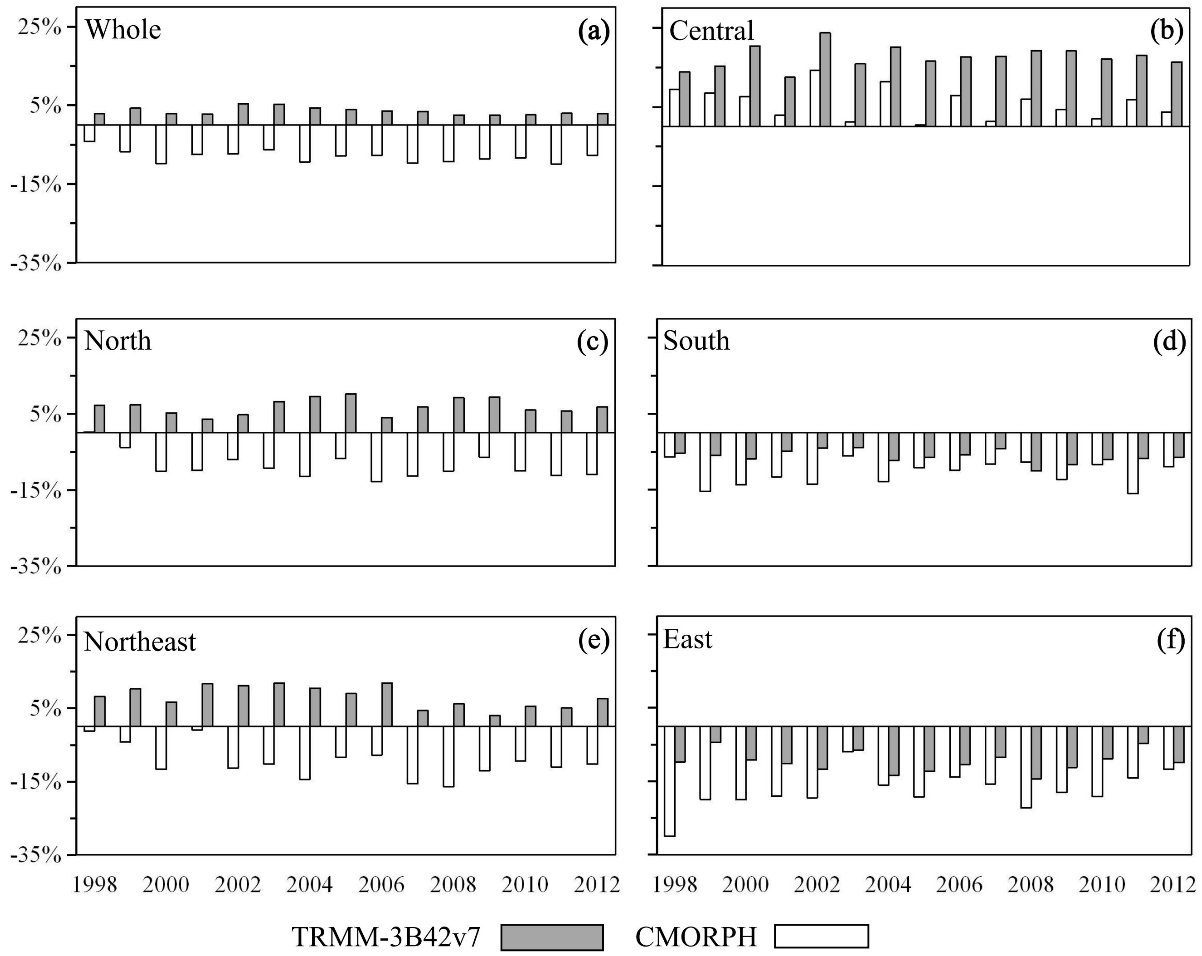

Figure 3. Relative errors of the annual CMORPH and TRMM-3B42v7 precipitation (%) for the various regions: (a) whole of Thailand, (b) Central Thailand, (c) North Thailand, (d) South Thailand, (e) Northeast Thailand, and (f) East Thailand.

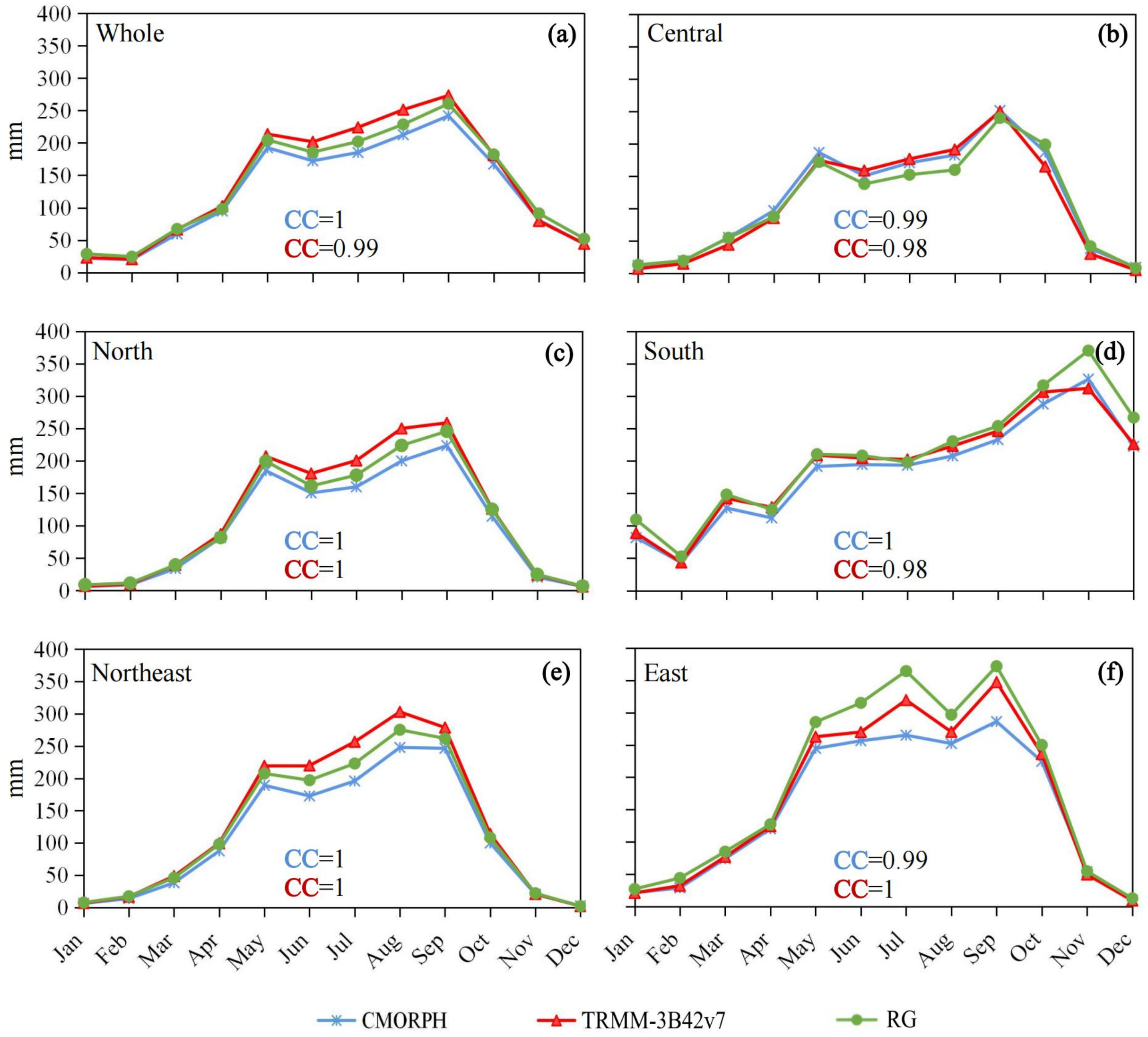

Figure 4. 15-yr averaged monthly (accumulated) precipitation (CMORPH, TRMM-3B42v7, and RG; mm) for the various regions: (a) whole of Thailand, (b) Central Thailand, (c) North Thailand, (d) South Thailand, (e) Northeast Thailand, and (f) East Thailand. RG=rain gauge, CC=correlation coefficient.

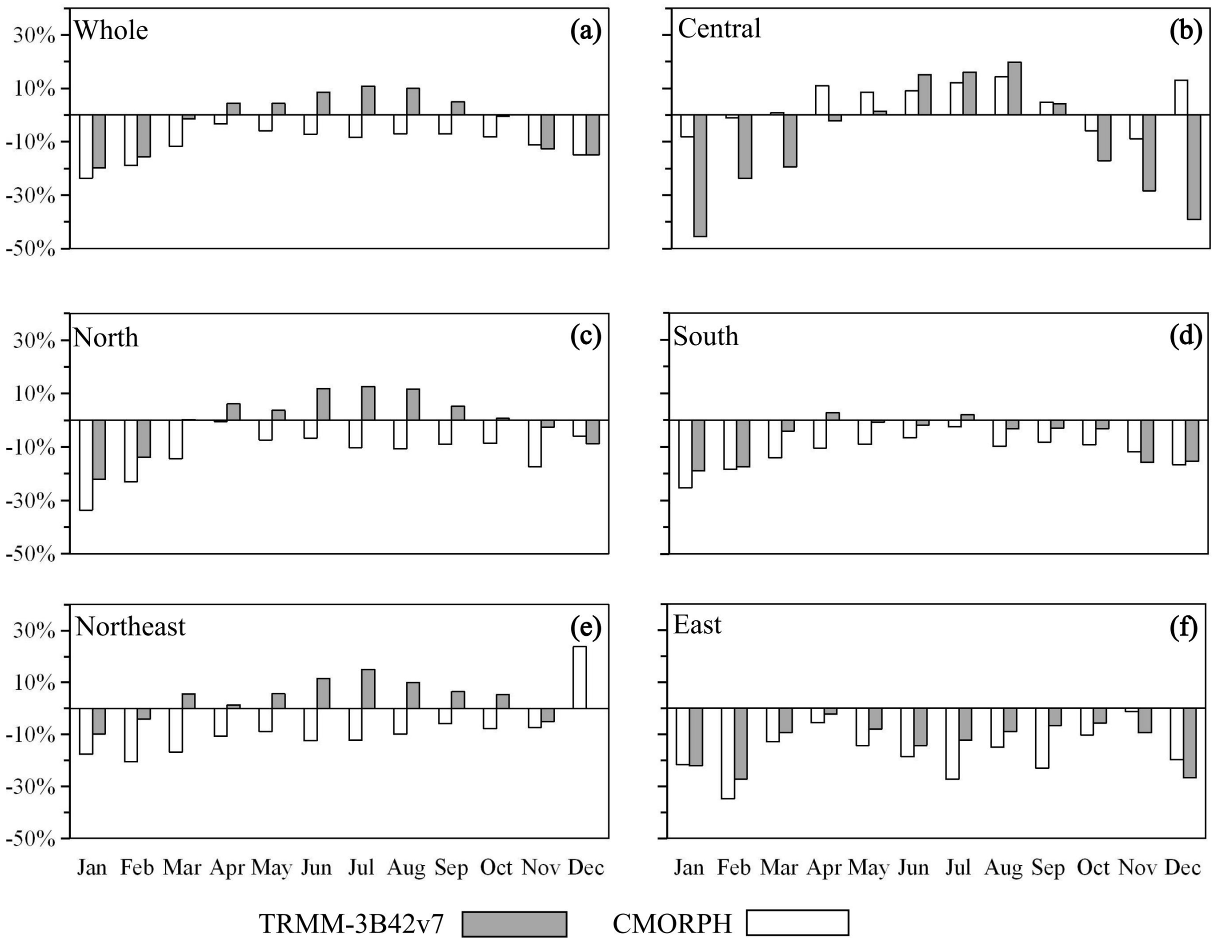

Figure 5. Relative errors of the 15-yr averaged monthly CMORPH and TRMM-3B42v7 precipitation (%) for the various regions: (a) whole of Thailand, (b) Central Thailand, (c) North Thailand, (d) South Thailand, (e) Northeast Thailand, and (f) East Thailand.

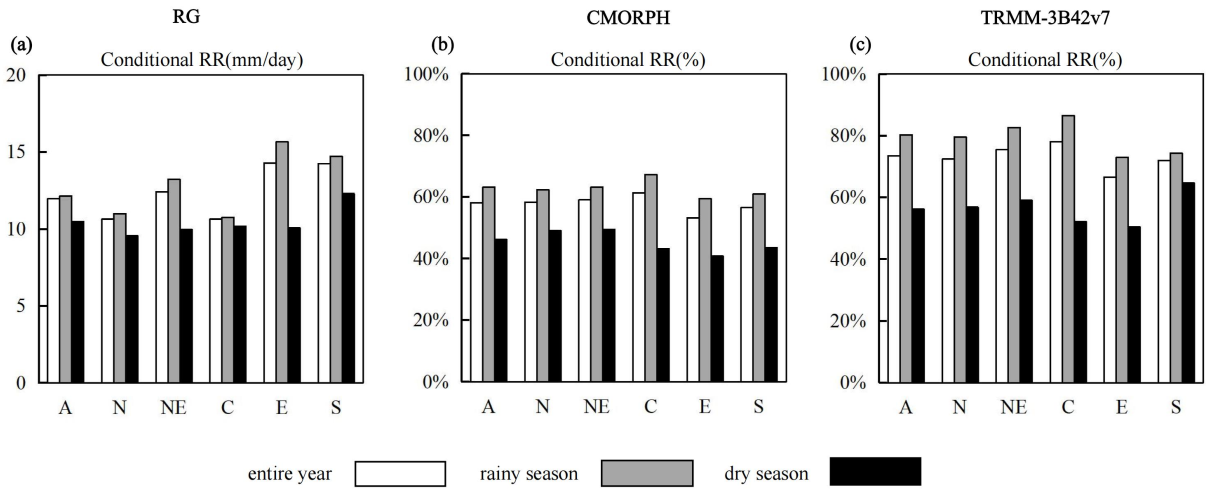

Figure 6. (a) RG-based mean conditional rain rate (CRR; mm day−1) of precipitation events for various regions during different periods (include entire year, rainy season and dry season). (b) and (c) Ratio of the CRR for CMORPH and TRMM-3B42v7 to that for RG, respectively (%). RG=rain gauge, A=all regions, N=North Thailand, NE=Northeast Thailand, C=Central Thailand, E=East Thailand, S=South Thailand.

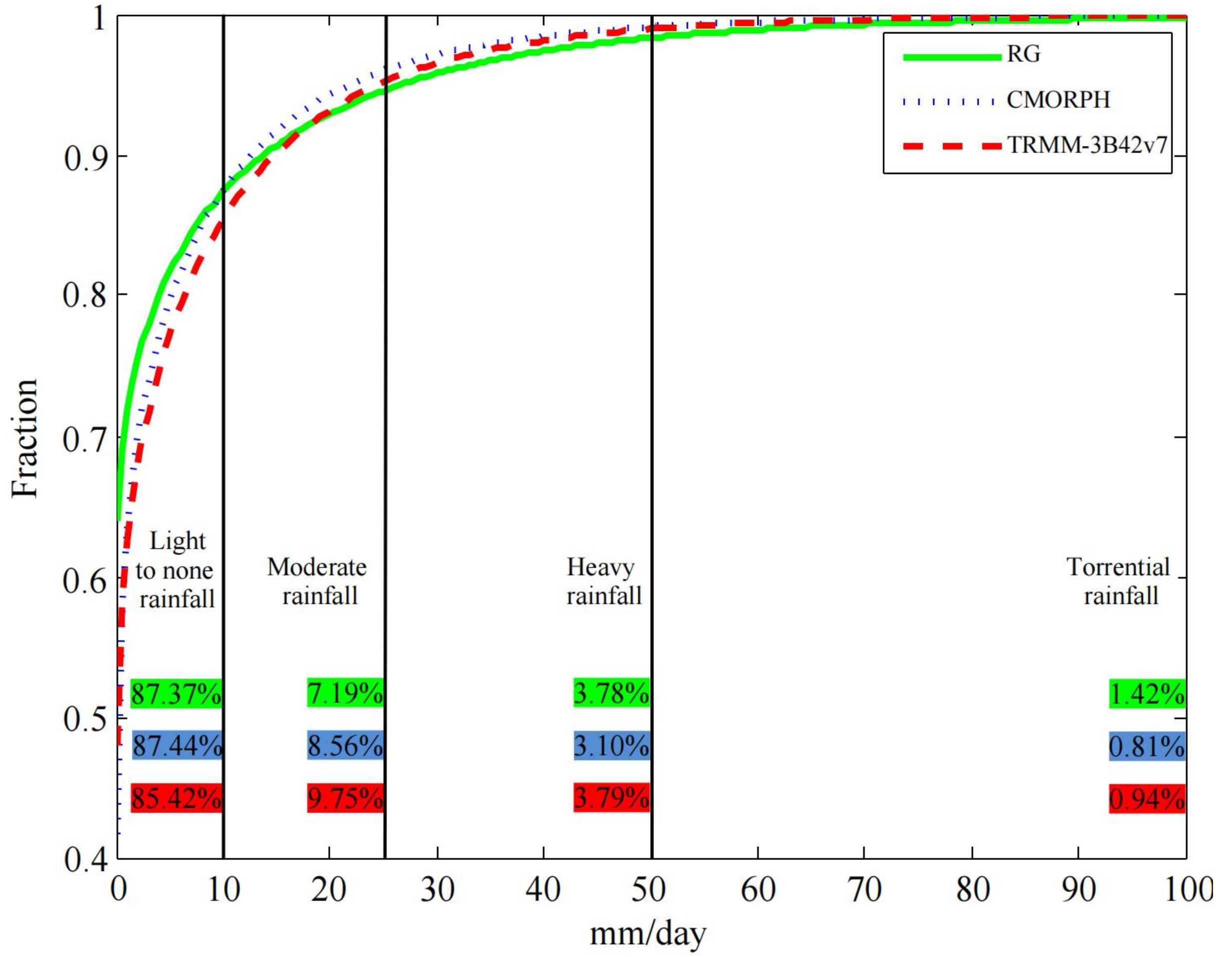

Figure 7. Cumulative distribution functions of the daily precipitation at the 91 stations during the 15-yr period (498,589 samples for each dataset) derived from the RG, CMORPH, and TRMM-3B42v7 data, where the three solid black lines divide the precipitation into four categories (i.e., light to none, moderate, heavy, and torrential rainfall) according to intensity. The proportions of the four precipitation categories for three types of precipitation data are indicated in different colors, where green represents RG, blue represents CMORPH, and red represents TRMM-3B42v7. RG=rain gauge.

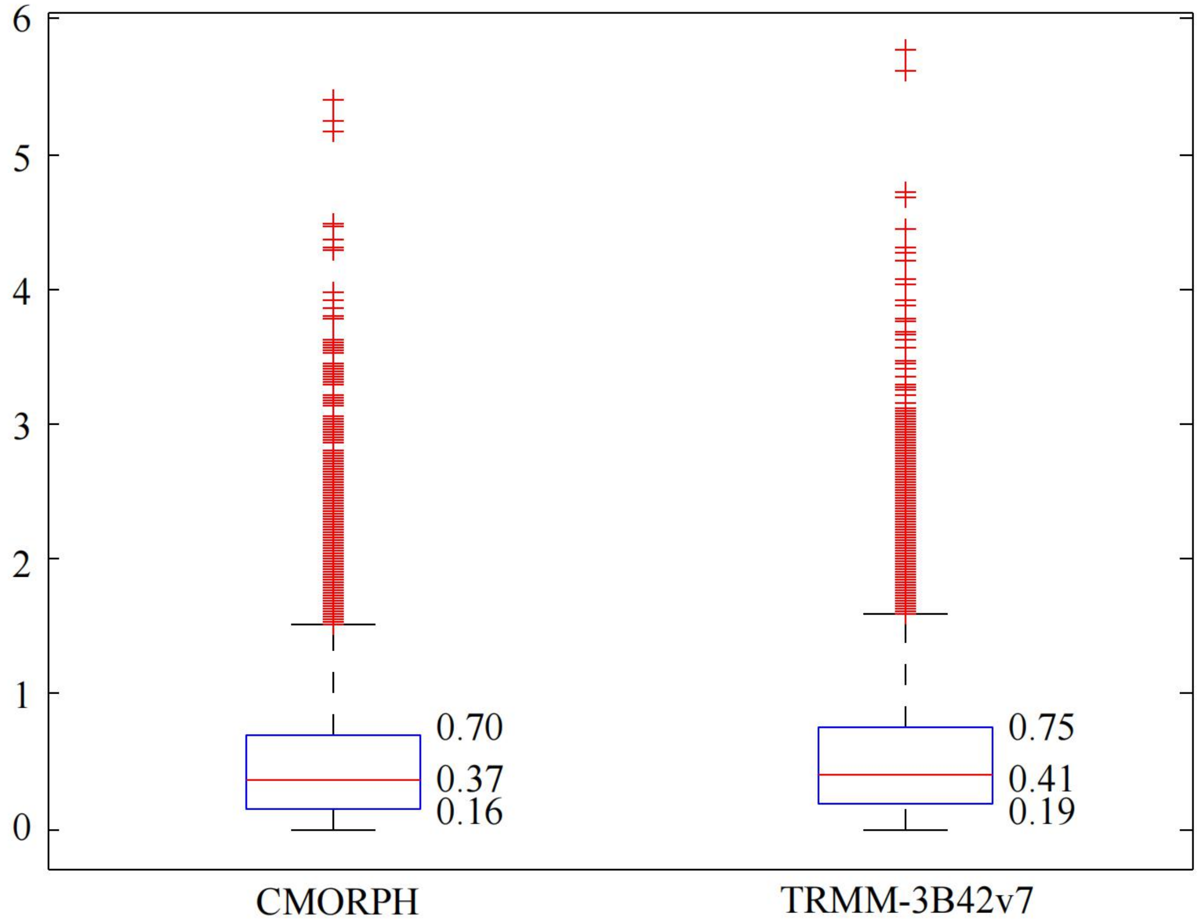

Figure 8. Boxplot of the ratio of the satellite data to RG-observed data for extreme precipitation (first 5% in the ranking of precipitation intensity based on total samples of 91 stations). The boxes indicate the 25th (Q1) to 75th (Q3) percentiles and the red line indicates the median value. The whiskers indicate the range of [Q1−1.5×(Q3−Q1)] or the minimum of the data (if all values in the data are bigger than the value calculated by the above expression) and [Q3+1.5×(Q3−Q1)] or the maximum of the data (if all values in the data are smaller than the value calculated by the above expression). RG=rain gauge.

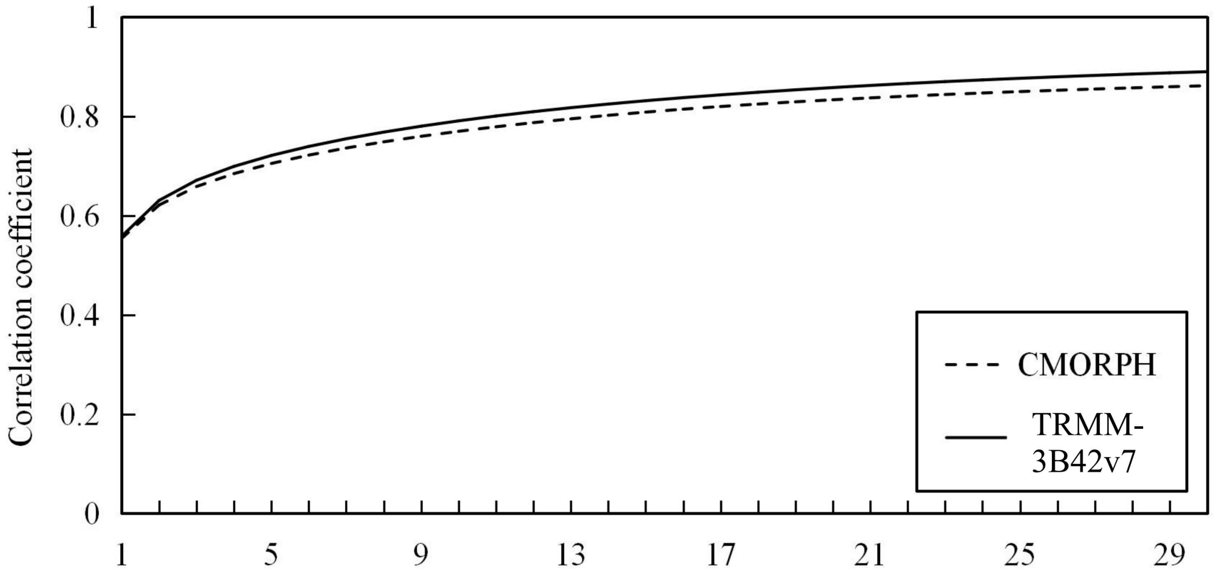

Figure 9. Linear correlation coefficients between the running means (the window size used for the running means are indicated in the abscissa) of the RG and satellite precipitation data (CMORPH/TRMM-3B42v7). RG=rain gauge.

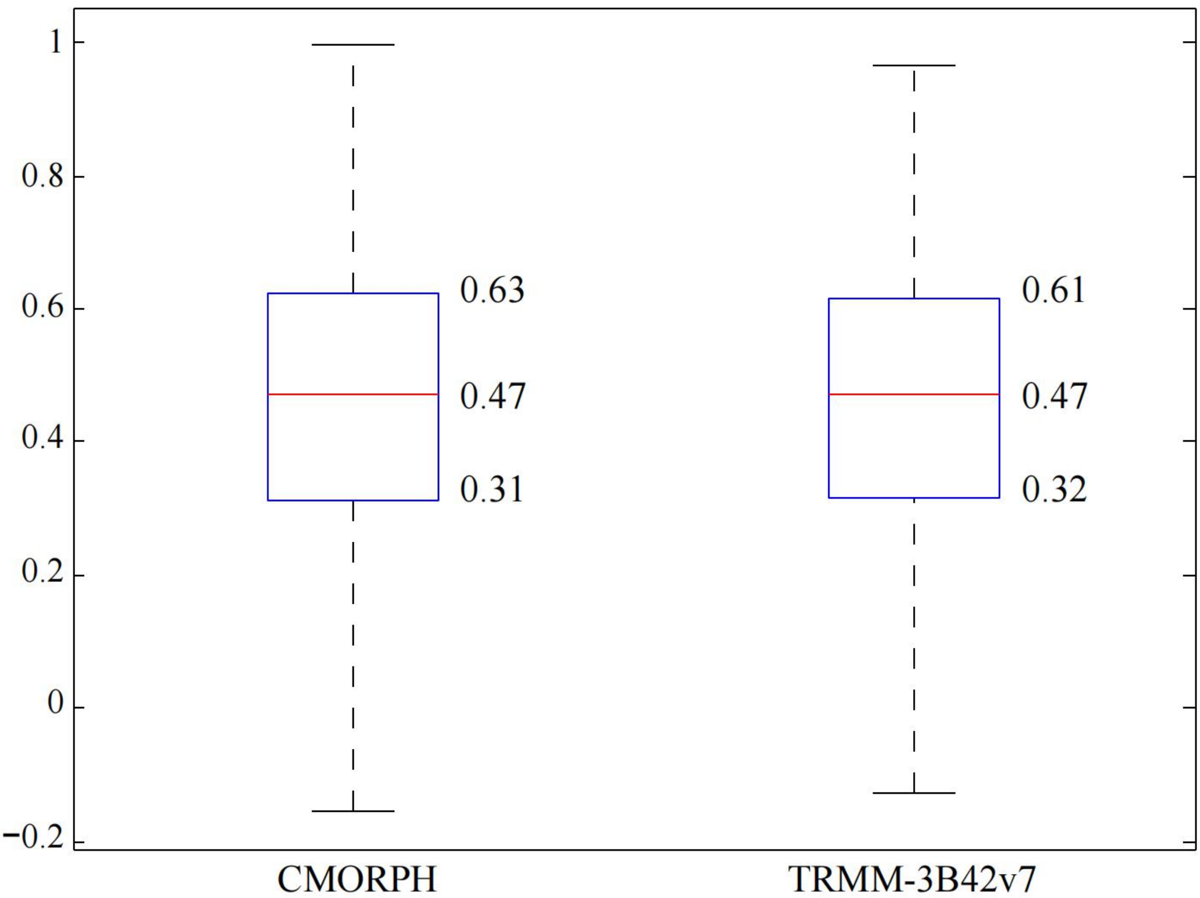

Figure 10. Boxplot of the spatial correlation between the satellite data (CMORPH/TRMM-3B42v7) and RG observations during the 15-yr period. The boxes indicate the 25th (Q1) to 75th (Q3) percentiles and the red line indicates the median value. The whiskers indicate the range of [Q1−1.5×(Q3−Q1)] or the minimum of the data (if all values in the data are bigger than the value calculated by the above expression) and [Q3+1.5×(Q3−Q1)] or the maximum of the data (if all values in the data are smaller than the value calculated by the above expression). RG=rain gauge.

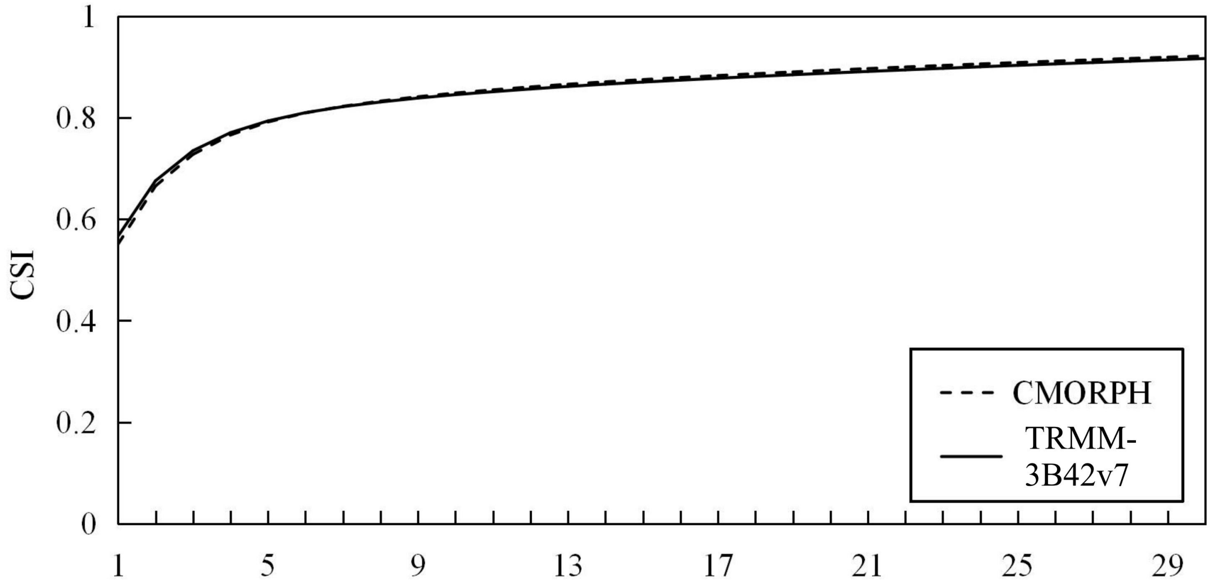

Figure 11. Critical success index (CSI) for CMORPH and TRMM-3B42v7 as a function of the number of days used for the running mean (abscissa).

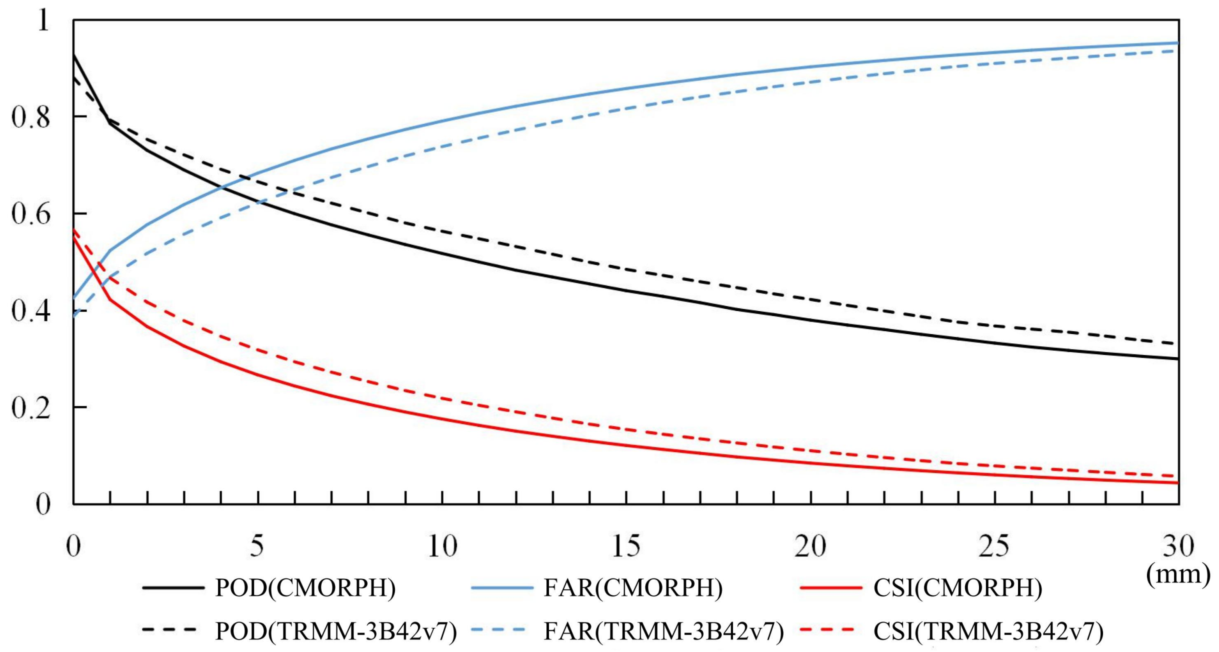

Figure 12. Probability of detection (POD), false alarm rate (FAR), and critical success index (CSI) for CMORPH and TRMM-3B42v7 relative to the rainfall intensity (the values in the abscissa indicate that the POD, FAR, and CSI values were calculated using rainfall intensities above that value) during the 15-yr period for the whole of Thailand.

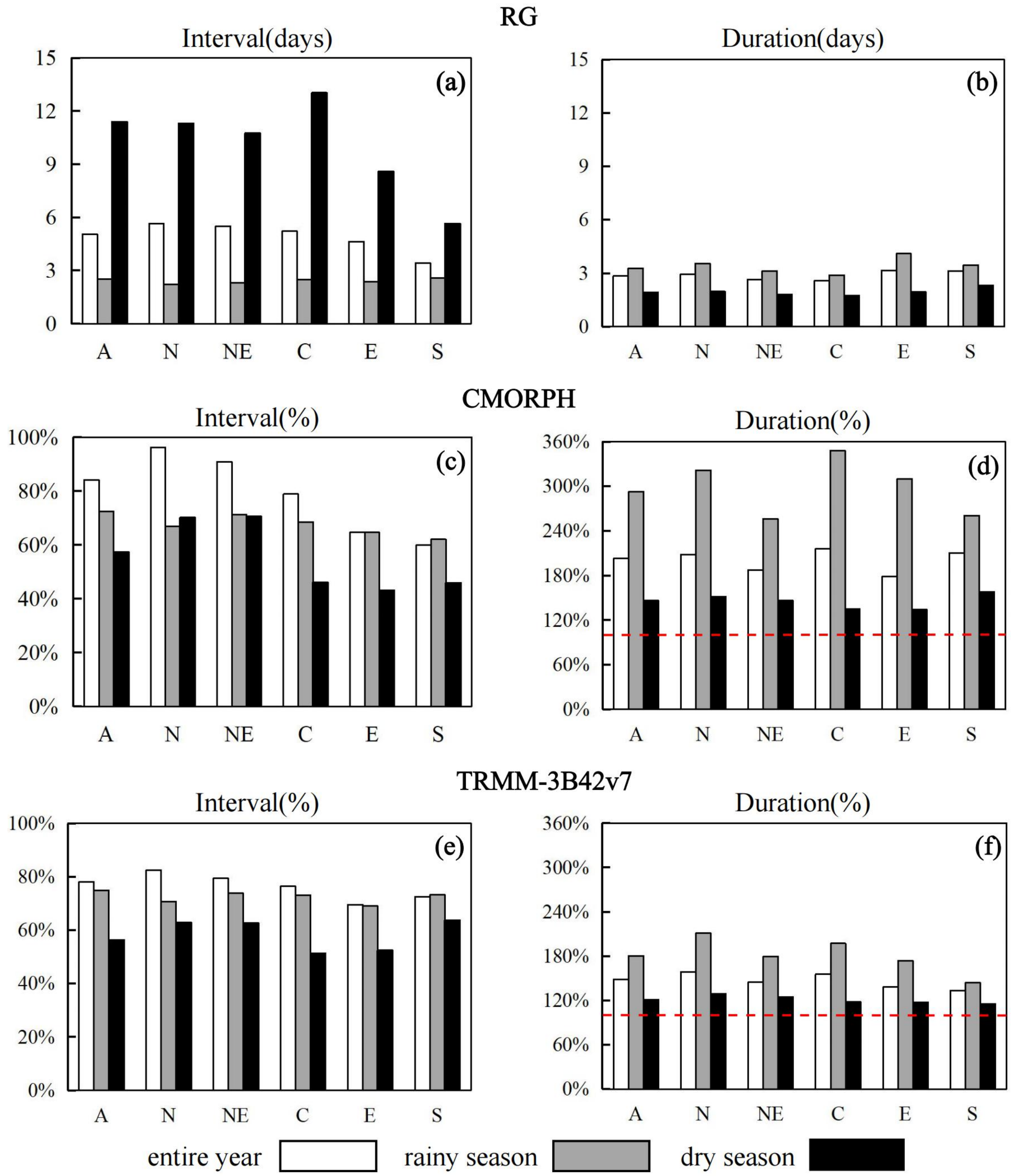

Figure 13. (a) RG-based mean precipitation interval (days) and (b) duration (days) for precipitation events in the various regions during different periods. (c) and (d) Ratio of the mean interval and duration for CMORPH to those for RG, respectively (%). (e) and (f) Ratio of the mean interval and duration for TRMM-3B42v7 to those for RG, respectively (%). The

red dotted horizontal line is at 100%. RG=rain gauge, A=all regions, N=North Thailand, NE=Northeast Thailand, C=Central Thailand, E=East Thailand, S=South Thailand.

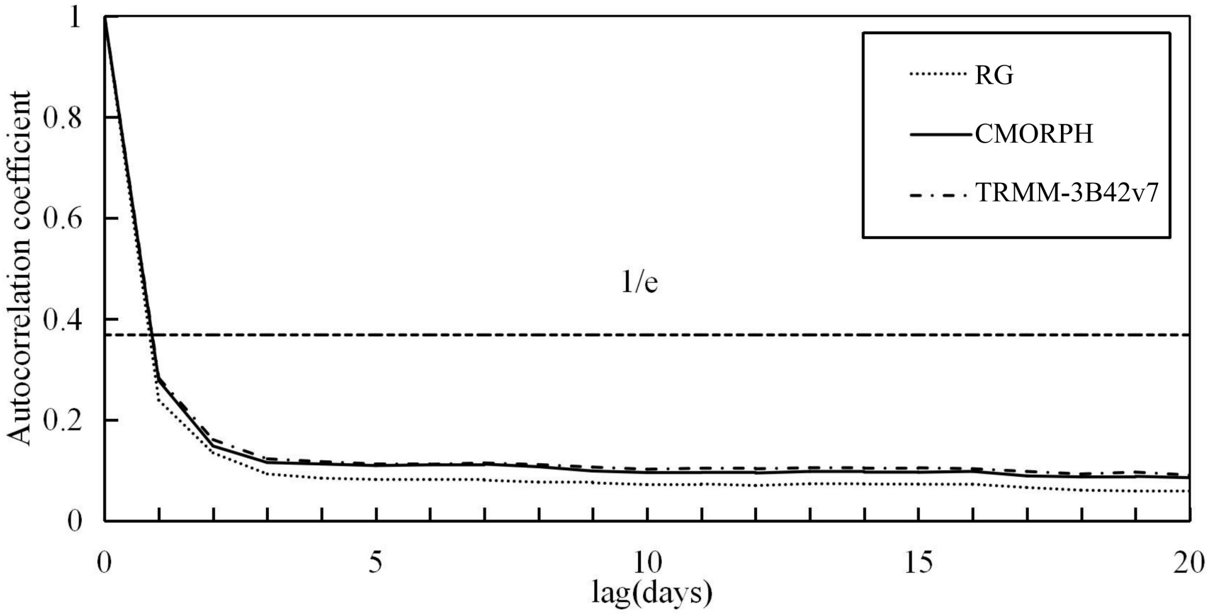

Figure 14. Temporal autocorrelation coefficients for RG, CMORPH, and TRMM-3B42v7. RG=rain gauge.